Phosphorus retention and event-scale nutrient dynamics in a constructed wetland

Insights from high-frequency sensor monitoring

Matthias Nikel

Degree project/Independent project • 30 credits
Swedish University of Agricultural Sciences, SLU
Faculty of Natural Resources and Agricultural Sciences
Department of aquatic sciences and Assessment
EnvEuro: Environmental Science - Soil, Water and Biodiversity
Uppsala 2026

Phosphorus retention and event-scale nutrient dynamics in a constructed wetland: Insights from high-frequency sensor monitoring

Matthias Nikel

Supervisor:	**Pia Geranmayeh, SLU, Department of aquatic sciences and Assessment**
Assistant supervisor:	Emma Lannergård, SLU, Department of aquatic sciences and Assessment
Assistant supervisor:	Günter Langergraber, BOKU, Department of Landscape, Water and Infrastructure
Examiner:	Martyn Futter, SLU, Department of aquatic sciences and Assessment

Credits:	30 ECTS
Level:	Second cycle, A2E
Course title:	Master thesis in Environmental science, A2E
Course code:	EX0897 VT2026
Programme/education:	EnvEuro: Environmental Science - Soil, Water and Biodiversity
Course coordinating dept:	Department of Aquatic Sciences and Assessment
Place of publication:	Uppsala
Year of publication:	2026
Cover picture:	Matthias Nikel
Copyright:	Matthias Nikel
Keywords:	Constructed wetland, Phosphorus retention, High-frequency monitoring, turbidity, Event-scale

Swedish University of Agricultural Sciences
Faculty of Natural Resources and Agricultural Sciences
Department of aquatic sciences and Assessment

Abstract

Constructed wetlands are widely promoted as edge-of-field measures to reduce nutrient and sediment losses from agricultural catchments, yet their event-scale retention performance remains poorly defined. Conventional monitoring approaches, based on grab sampling or flow-proportional sampling, are costly and typically lack the temporal resolution. That is needed to capture the short-lived, high-concentration pulses that can drive the bulk of annual nutrient transport.

In this study, high-frequency (HF) in situ sensors measured turbidity, fluorescent dissolved organic matter (fDOM) and nitrate and were deployed at the inlet and outlet of a small phosphorus retention wetland in a tile-drained clay catchment in east-central Sweden. Fortnightly grab samples were collected and used to establish site-specific turbidity–total phosphorus (TP) and fDOM–dissolved organic carbon (DOC) regression relationships, enabling continuous concentration and load estimates throughout the monitored period. Six events, spanning early winter to spring snowmelt, were identified and analysed with respect to hydraulic loading, inlet–outlet concentration dynamics, concentration-discharge hysteresis, and hydraulic and concentration lags.

Turbidity proved a strong proxy for TP ($R^2 = 0.93$, $n = 13$), while the fDOM–DOC relationship was weaker ($R^2 = 0.23$, $n = 15$) and less reliable for load estimation. The wetland acted as a TP sink during four of the six events, while two events showed net P export, indicating that retention performance varied considerably between events, although the event definition was not representative for all actual field conditions. Hydraulic lags (Q-lag) between inlet and outlet peaks deviated from the theoretical water residence time (τ_{th}) in several events, indicating short-circuiting and variable effective wetland volume. Concentration-discharge hysteresis differed between inlet and outlet and between events, revealing distinct differences in source dynamics and internal sediment mobilisation. Nitrate monitoring could not be completed quantitatively due to sensor drift.

These findings demonstrate that HF sensor-based monitoring can resolve event-scale processes in agricultural wetlands that remain invisible to conventional sampling, and that hydraulic loads (HL) and effective volume (V_{eff}) are critical determinants of short-term TP retention performance.

Keywords: Constructed wetland, phosphorus retention, high frequency monitoring, in-situ sensors, turbidity, event-scale

Acknowledgements

My sincere thanks go to my supervisors, Pia and Emma, for supporting me throughout this thesis and for giving me the opportunity to find solutions on my own without ever leaving me on my own. Their enthusiasm for wetlands was especially helpful during the difficult field situations in winter.
Special thanks are due to Maria, who helped me in the field and taught me a bit about Sweden during our drives to and from the wetland.

I am especially grateful to my Master colleagues, friends and family, and most of all to my parents. Without their support, not only financially, I would not have been able to complete my studies, even if they claim otherwise. I know this support is not something that can be taken for granted.

"Wasser ist die Grundlage des Lebens!"

- Hans Heger

AI-based tools (large language models) were used during the writing process to refine English wording, sentence structure and to obtain suggestions on the overall thesis structure and text flow. Additionally, it was used as aid for visualising a concept used.
Decisions on content, method, data analysis and interpretation were made by the author, and all final text was checked and approved by the author.

Table of contents

List of tables

List of figures

Abbreviations

Abbreviation	Description
C	Carbon
conc.-lag	concentration lag
DOC	Dissolved organic Carbon
fDOM	Fluorescent dissolved organic matter [QSU]
FNU	Formazin Nephelometric Units (Turbidiy Unit EXO2)
HELCOM	HELCOM – Helsinki Commission (Baltic Marine Environment Protection Commission)
HF	High-frequency (monitoring)
HL	Hydraulic load
L	Load
N	Nitrogen
OrgN –	Organic nitrogen
P	Phosphorus
PP	Particulate phosphorus
Q	Discharge / water flow
Q-lag	hydraulic / discharge lag
QSU	Quinine Sulfate Units (fDOM Unit EXO2)
SLU	SLU – Swedish University of Agricultural Sciences
SMHI	Swedish Meteorological and Hydrological Institute
TOC	Total organic Carbon
TP	Total phosphorus
V_{eff}	Effective wetland volume
WRT / τ_{th}	Water residence time / theoretical hydraulic residence time

1. Introduction

Nutrients such as phosphorus (P) and nitrogen (N) are essential for agricultural production, but losses from fields to surface waters contribute to eutrophication and declining water quality in rivers, lakes and coastal ecosystems such as the Baltic Sea (HELCOM, 2023). Elevated nutrient inputs promote algal blooms, oxygen depletion and biodiversity loss. This has led to international and European policy responses, including the HELCOM Baltic Sea Action Plan and the EU Water Framework Directive (HELCOM, 2023; European Commission, 2024).

Constructed wetlands are widely used as edge-of-field measures to intercept nutrients in agricultural runoff and drainage water before they reach downstream waters (Kynkäänniemi, 2014). By reducing flow velocity and increasing hydraulic residence time, they create conditions that favour nutrient retention (Mendes, 2020). For P, the main retention processes are sedimentation and burial in bottom sediments of particle-bound P. However, P stored in sediments can also be remobilised or released again under changing conditions. Dissolved reactive P may be retained by sorption to Fe/Al/Ca sorbents, while internal loading from mineralization, desorption or redox-driven release (e.g., reduction of Fe oxides) can drive re-mobilisation of sediment P (Mendes, 2020).

For carbon (C), retention occurs through accumulation of organic matter and reduced decomposition under wetland conditions (Mendes, 2020; Land et al., 2016).

For nitrogen, the main removal pathway in agricultural wetlands is denitrification, while plant and microbial uptake can also contribute, although this storage is often temporary unless biomass is removed from the wetland (Mendes, 2020).

Retention performance for both P and N is highly variable. It depends strongly on hydrological conditions as well as on the magnitude and form of nutrient loading (Land et al., 2016). Wetlands with relatively high nutrient input can therefore function effectively, but only if their hydraulic loading (HL) and flow residence time remain within a range that still allows retention. In small wetlands with high HL, performance can become more variable and event-driven export may occur, particularly when internal sediment stores are mobilised (Kynkäänniemi, 2014).

Short runoff peaks and snowmelt events can deliver large nutrient loads over a short time but also reduce residence time and increase turbulence. Under these high hydraulic loading conditions, retention of new sediments is weakened and resuspension of previously accumulated sediments. and associated phosphorus promoted (Braskerud, 2002; Kynkäänniemi, 2014). As a result, wetlands may act as nutrient sinks during some periods but shift towards net export during others (Kynkäänniemi, 2014; Mendes, 2020).

The key question is if the wetland retains or releases nutrients over time. Nutrient retention performance is commonly evaluated using inflow–outflow mass balances, which require both discharge and concentration data at suitable temporal resolution (Kynkäänniemi, 2014, Ulén et al., 2019). Concentration describes the amount of nutrient per unit volume of water, whereas load represents the total transported mass. Therefore, is load the parameter needed to quantify actual nutrient export or retention (Mendes, 2020). In other words, concentration is useful for characterising water quality, but load is required to determine whether the wetland functions as a sink or source (Mendes, 2020).

Reliable evaluation of wetland performance requires monitoring that captures both, long-term averages and short-term changes. Water quality monitoring based on flow-proportional composite sampling is useful for estimating longer-term loads, but it might not capture rapid concentration changes or short-lived peaks during individual events (Rode et al., 2016). To follow wetland performance during short-lived hydrological events high-frequency (HF) monitoring is needed.

High-frequency in-situ sensors are increasingly used in surface-water monitoring (Bieroza et al., 2023). They provide continuous measurements of turbidity, fluorescent dissolved organic matter (fDOM), chlorophyll, UV absorbance, electrical conductivity, dissolved oxygen, and temperature (Bieroza et al., 2023).

Optical measurements such as turbidity, fDOM and UV absorbance can act as proxies for key water-quality parameters, such as total phosphorus (TP) (Lannergård, 2016), dissolved organic carbon (DOC) (Hoffmeister, 2020) and nitrate (Pellerin et al., 2016), when calibrated against site-specific grab samples. This enables high-frequency monitoring, that can be used to estimate loads and retention, to characterise event-scale nutrient dynamics in constructed wetlands (Ulén et al., 2019). However, to date, most applications of turbidity, fDOM, and UV–nitrate sensors have been undertaken in riverine settings or lakes, with limited research in wetland setting (Jarvie et al., 2020; Koskiaho and Puustinen, 2019). High-resolution monitoring can improve understanding of nutrient dynamics in wetlands, including short-term biogeochemical responses and carbon-linked processes (Jarvie et al., 2020). However, Jarvie et al. (2020) focus on nutrient dynamics inferred from high-resolution chemical and metabolic measurements, whereas the aim here is to exploit simple, optical in situ measurements as easily deployable proxies for these dynamics, with an emphasis on hydraulics rather than wetland metabolism.

Therefore, the present study applied high-frequency monitoring to a small constructed wetland aiming at retaining P from an agricultural area to improve understanding of retention performance under event-driven hydrological conditions. In addition, it evaluated whether HF turbidity, fDOM, and nitrate measurements can enhance the interpretation of P, C, and N dynamics.

The study addresses the following questions:

1. To what extent can turbidity, fDOM, and nitrate sensor measurements act as proxies for TP, DOC, and nitrate concentrations, based on site-specific calibration against laboratory data?

2. Under which hydrological conditions does the wetland show effective TP retention, and under which circumstances does retention appear to weaken?

3. How do inlet and outlet conditions differ during high-flow and baseflow periods, and what do the differences imply for wetland function?

4. What do event-scale hysteresis and inlet–outlet lags reveal about the internal processes that control P retention and export in the wetland?

2. Theory

2.1 Monitoring strategies for water quality

2.1.1 Inflow-outflow balances

Nutrient retention is defined as the difference between the mass entering and leaving the wetland over a given period, (equation I) (Braskerud, 2002). Nutrient loads (L) are calculated from water flow rate (Q) and concentration (conc.) over time for discrete time steps using equation II and III. following standard inflow–outflow mass-balance approaches (Kadlec and Wallace, 2009). Loads are computed at the inlet and outlet, and retention or release is quantified as the difference between inflow and outflow loads over the selected time window (Kynkäänniemi, 2014; Kadlec and Wallace, 2009).

$$Retention\,[\frac{g}{h}] = L_{in}[\frac{g}{h}] - L_{out}[\frac{g}{h}]$$ *Equation I*

$$L_{in}[\frac{g}{h}] = Q_{in}[\frac{m^3}{h}] * conc_{in}[\frac{g}{m^3}]$$ *Equation II*

$$L_{out}[\frac{g}{h}] = Q_{out}[\frac{m^3}{h}] * conc_{out}[\frac{g}{m^3}]$$ *Equation III*

A high concentration does not necessarily imply a high load if discharge is low, while a moderate concentration can still generate a large load under high-flow conditions (Bieroza et al., 2023).

2.1.2 Event-scale lags and wetland residence time

Theoretical residence time (τ_{th}) and HL

A common way to characterise wetland hydraulics is the theoretical residence time (τ_{th}), defined as in equation IV (Persson et al., 1999). In a simplified reactor view, this value represents the average time a parcel of water would spend in the system if water were perfectly mixed or flowed as an ideal plug. τ_{th} is widely used in wetland design and performance assessments, as it connects retention capacity to simple hydraulic measures such as volume and inflow (Kadlec and Wallace, 2009).

For a time-varying inflow, the τ_{th} can be written as equation IV. However, it does not account for internal flow heterogeneity, preferential flow paths, or dead zones, however, actual travel times may deviate substantially from this theoretical estimate (Kadlec and Wallace, 2009). Some water parcels may shortcut rapidly along high-velocity flow paths, whereas other parcels are retained much longer in slowly exchanging zones, so that the effective volume participating in throughflow is smaller than the geometric volume and the true mean residence time is shorter than τ_{th}.

The hydraulic load (HL) is defined as the Q at the inlet devided by the wetland surface area (equation V) and represents the primary driver of hydraulic conditions and nutrient retention performance in constructed wetlands (Kadlec and Wallace, 2009).

$$\tau_{th}(t)[h] = \frac{V_{eff}[m^3]}{Q_{in}(t)[\frac{m^3}{h}]}$$ *Equation IV*

$$HL[\frac{m}{h}] = \frac{Q_{in}(t)[\frac{m^3}{h}]}{A_w[m^2]}$$ *Equation V*

Travel-time estimate (centroid based lag)

Because water parcels need a finite and variable time to travel through the wetland, changes in flow at the inlet are not reflected immediately at the outlet. Accounting for these lags is essential when matching inflow events or time slices to their corresponding outflow responses in the mass balance, because travel-time differences can mask the true hydrologic and hydraulic behaviour of the wetland (Persson et al., 1999).

Centroid-based lag and travel-time definitions provide a robust way to describe delays in hydrologic response, commonly used as the time interval between the flow-weighted centroid of excess precipitation and the flow-weighted centroid of runoff (Gericke and Smithers, 2013). In the US Department of Agriculture Natural Resources Conservation Service (NRCS), this lag concept is related to the time of concentration and is used to characterise watershed response times (USDA NRCS, 2010). By analogy, the same centroid-based framework can be applied to paired inflow and outflow hydrographs in wetlands. The lag is estimated from the difference between the flow-weighted centroids of inlet and outlet discharge (Figure 1)(equation VI, VII, VIII). This provides an event-scale empirical travel-time measurement consistent with observed hydrograph shapes. "This approach is similar to Ulén et al. (2019), who estimated hydraulic lag from hydrograph peak timing at the inlet and outlet."

$$t_{\text{mean,in}}[h] = \frac{\sum(t[h] \cdot f(conc_{in}[\frac{g}{m^3}]; Q_{\text{in}}[\frac{m^3}{h}]))}{\sum f(conc_{in}[\frac{g}{m^3}]; Q_{\text{in}}[\frac{m^3}{h}])} \qquad \textit{Equation VI}$$

$$t_{\text{mean,out}}[h] = \frac{\sum(t[h] \times f(conc_{out}[\frac{g}{m^3}]; Q_{\text{out}}[\frac{m^3}{h}]))}{\sum f(conc_{out}[\frac{g}{m^3}]; Q_{\text{out}}[\frac{m^3}{h}])}$$

$$\text{Lag[h]} = t_{\text{mean,out}}[h] - t_{\text{mean,in}}[h]$$

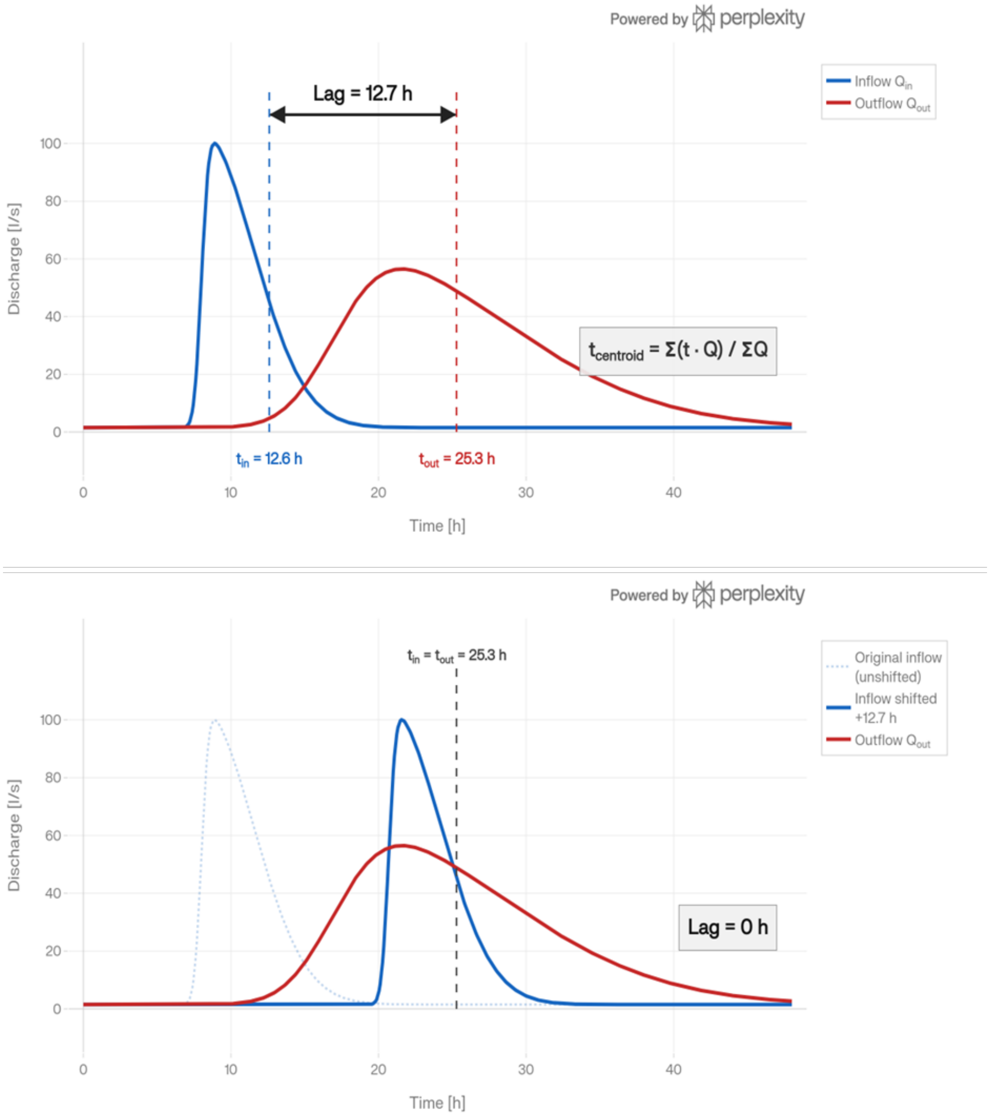

Figure 1 - visualization of the centroid mrthod for lag estimation (Source AI Perplexity)

Differences between hydraulic and concentration lags

In wetlands and ponds, residence-time distributions and tracer response curves can be used to estimate mean detention times and effective volumes, thereby linking observed lags to hydraulic efficiency and internal flow patterns (Wahl et al., 2010). Concentration responses can be further delayed or prolonged by internal processes such as settling, resuspension, sorption, and transformation, so that the timing of solute export does not necessarily follow the hydraulic response (Bieroza et al., 2023).

Hysteretic concentration–discharge patterns provide an additional way to diagnose these processes, because they capture differences in the timing and rate of change of concentration and discharge on the rising and falling limbs of events (Bieroza et al., 2023). Such hysteresis patterns can help identify the timing and direction of solute and particulate mobilisation and delivery, and when combined with hydraulic lag (Q-lag) and concentration lag (conc.-lag) estimates they support a more detailed interpretation of internal wetland storage and processing (Bieroza et al., 2023).

2.2 Optical sensors for water quality

Optical sensors work by emitting light at specific wavelengths and measuring how much of this light is scattered or absorbed in the water. Turbidity sensors mainly detect backscattered light from suspended particles, so increasing particle concentrations produce stronger scattering signals (Bieroza et al., 2023). UV– and FDOM- sensors exploit the optical properties of coloured dissolved organic matter (CDOM), using its absorbance and fluorescence as proxies for DOC concentrations (Lee et al., 2015). These light responses can be calibrated against laboratory analyses, allowing the use of continuous proxy estimates of suspended solids, TP, DOC, and nitrate to be derived from the sensor signals (Bieroza et al., 2023).

At high turbidity and during high-flow events, turbidity-based proxy relationships can become less reliable, so careful calibration and quality control are needed (Lannergård et al., 2019).

Monitoring strategies and sensor configurations should be tailored to the specific scientific questions, required temporal resolution, and local hydrological and biogeochemical conditions, rather than being chosen solely based on cost or convenience (Bieroza et al., 2023).When appropriately designed and quality-assured, optical HF sensors provide near-continuous time series that reveal event-scale dynamics. These short-lived peaks provide insight, which low-frequency grab or composite sampling cannot resolve (Bieroza et al., 2023).

2.2.1 Turbidity as a proxy for P

Turbidity, measured as light scattering by suspended particles, is widely used as a proxy for P because suspended sediment often carries a substantial fraction of particulate P (PP). Some studies calibrate turbidity directly against TP, while others focus on PP (Jones et al., 2011). Turbidity sensors typically rely on one or a few fixed optical bands and measure scattered light at one or two angles (Bieroza et al., 2023). When particulate forms dominate and sufficient calibration data are available, site-specific regressions between turbidity and TP or PP typically provide good fits. Turbidity therefore serves as a useful surrogate for event-scale phosphorus dynamics, including concentration changes, high-flow P loads, and short-term retention or export (Jones et al., 2011; Villa et al., 2019).

2.2.2 fDOM as a proxy for DOC

Fluorescence sensors targeting fDOM enable continuous tracking of DOC dynamics and export (Hoffmeister et al., 2020). These sensors use a defined excitation–emission pair to detect fluorescence from coloured dissolved organic matter, with stronger fDOM signals generally indicating higher DOC (Lee et al., 2015). Because the fluorescence response depends on local water chemistry, particle properties, and sensor design, site-specific calibration against grab samples is required to convert fDOM readings to DOC and to correct for interferences such as temperature, turbidity, inner-filter effects, and instrumental drift (Hoffmeister et al., 2020).

2.2.3 Nitrate sensors

Optical nitrate sensors exploit the strong UV absorbance of nitrate in the 200–250 nm band to provide HF nitrate concentrations. UV nitrate sensors range from simple single- or dual-wavelength devices to full-spectrum spectrophotometers (Pellerin et al., 2016). In principle, the sensor passes UV light through a defined optical path and quantifies how much light is absorbed by nitrate; the resulting absorbance is then converted to concentration using calibration relationships (Pellerin et al., 2016).

3. Method

The study applied a lumped empirical mass balance framework to evaluate retention and export dynamics at the wetland scale with focus on P. Retention was calculated as the difference between inflow and outflow load. The approach did not explicitly simulate internal physical or biogeochemical processes but infers system behaviour from observed flux differences and allows for the use of proxies regarding nutrient estimations.

3.1 Site description

The Nybble wetland (Figure 2) was chosen for this study because existing flow-proportional monitoring have shown periods of nutrient release and it represents a small, farmed clay-soil catchment where HF monitoring can resolve event-scale P dynamics. The wetland was constructed in 2010–2011 to reduce P loads to the River Kilaån in east-central Sweden, which discharges into the Baltic Sea (Kynkäänniemi, 2014).

The catchment area has a size of 77 ha, with mainly forest (about 55%) and tile-drained arable land (about 39%) on clay-rich soils (mean clay content 22%) (Kynkäänniemi, 2014). The average slope is 4.7%, making the area prone to erosion and PP losses (Kynkäänniemi, 2014). Soil P status is moderate (75 mg P-AL kg^{-1}). The absence of livestock, combined with subsurface drainage and macropore flow, makes Nybble representative of many intensively cultivated clay catchments in southern and central Sweden. Such catchments are known to contribute disproportionately to P losses in the region (Kynkäänniemi, 2014). The wetland was positioned according to the critical source area concept, intercepting tile-drain and surface runoff from a known high-risk drainage ditch, thereby maximising incoming P load per unit wetland area (Kynkäänniemi, 2014).

Nybble was explicitly designed as a small P-wetland optimised for particle-bound P retention, with a 1 m deep inlet sedimentation basin followed by a shallow (0.3 - 0.4 m) downstream section (Kynkäänniemi, 2014). The inlet sedimentation basin was dredged in 2016 to remove accumulated material and maintain depth, while the shallow vegetated area has continued to infill gradually with P-rich sediment (Kynkäänniemi, personal communication, 2026). During this study, the shallow zone is covered with dense emergent vegetation and only a few centimetres of water level remain over much of the area.

The wetland has a long, narrow planform (length-to-width ratio of 11:1) to promote hydraulic efficiency. The Nybble wetland is small, with a surface area of

0.13% of the catchment. This ratio lies at the lower end of the recommended 0.1 - 0.5% range for P-wetlands and implies relatively high HL (Kynkäänniemi, 2014).

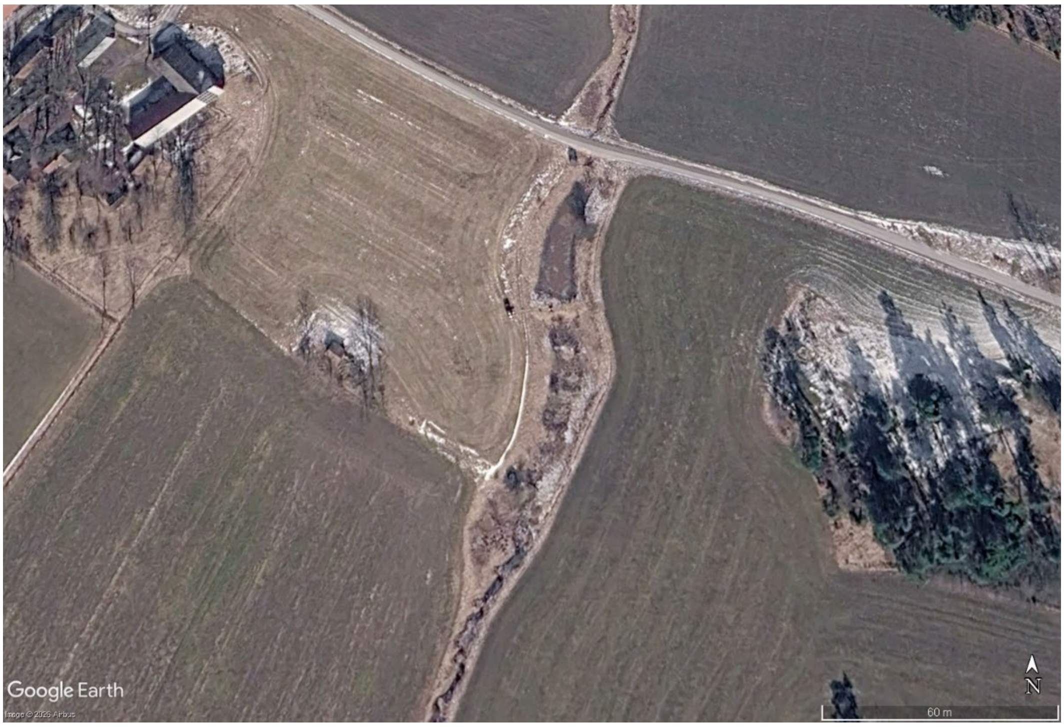

Figure 2 - Nybble wetland aerial view (58°44'49.07"N 16°41'03.63"E)(source: Google Earth)

3.2 Weather data

Daily weather data (air temperature, precipitation, and snow depth) were obtained from the Swedish Meteorological and Hydrological Institute (SMHI) for the period 14 November 2025 to 30 April 2026 (SMHI, 2026). Precipitation and snow depth were taken from the climate station Nyköping (no. 86660), located approximately 21 km from Nybble (SMHI, 2026). Daily mean air temperature was not available at this station and was therefore taken from the nearby station Kolmården-Strömsfors A (no. 86420) (SMHI, 2026). Snow depth from SMHI was used as a proxy for on-site conditions and to identify periods when field access and equipment operation were constrained by ice and snow cover (SMHI, 2026).

3.3 Discharge Data

Water level was continuously measured at V-notch weirs installed at both the inlet and outlet of the Nybble wetland (Kynkäänniemi, 2014). Upstream water level at each weir was recorded with pressure sensors, and established stage–discharge relationships for the specific V-notch geometry were used to convert water level to flow, following Kynkäänniemi (2014). The flow datasets were provided by the University Institute. The water levels at the weirs and sampling time were recorded for later discharge calculation and data verification. Side ditches and the outlet configuration ensure that essentially all runoff enters via the inlet and passes through the wetland (Kynkäänniemi, 2014). Therefore, both the historical monitoring by Kynkäänniemi (2014) and the present HF measurements are catchment-representative (Kynkäänniemi, 2014).

3.4 Water quality

The HF water quality monitoring was combined with water quality sampling during the research period in two-week intervals. These were cross checked and used for calibration.

3.4.1 Grab sampling

Fortnightly grab samples of water were collected at the V - notch weirs at the inlet and outlet of the wetland. At each visit, a single mid-stream sample was taken directly from the V - notch. The samples were transported to the geochemistry laboratory at the Swedish University of Agricultural Sciences (SLU), accredited according to ISO/IEC 17025, where they were analysed. Phosphate, TP, nitrite and nitrate, total nitrogen, total organic carbon (TOC), DOC, suspended solids (SS) and turbidity were derived following standard methods (SLU Geochemical Laboratory, 2024).

Water sample collection was more difficult during winter because ice accumulation restricted access to the water at the weirs. During parts of the winter season the samples had to be taken after removing the ice layer.

3.4.2 High-frequency measurement with EXO2 multiparameter sonde

High-frequency in situ monitoring was carried out using an EXO2 Multiparameter Sonde (YSI Inc., USA). Two EXO2 sondes were installed in perforated plastic pipes upstream of the V-notch weirs at the wetlands in- and outlet (Figure 3). This ensured that (i) measurements were representative of the cross-section, (ii) in situ data were directly comparable with laboratory-analysed samples, (iii) hydraulic and water-quality data were temporally synchronized, and (iv) flow velocity limited stagnation and biofouling effects, while preserving safe and efficient field access.

The sensors were first deployed on 14 November 2025. They were then removed between 20 November and 2 December due to emerging ice cover and redeployed on 2 December, remaining in place until 30 December, when winter conditions again required retrieval. Redeployment was not possible during mid-winter, and the final deployment therefore started on 2 March and lasted until 28 April. Throughout the study period, the site was visited at approximately two-week intervals to visually check flow conditions, and images from an installed camera at the outlet weir were used to detect possible thaw or flow events between the biweekly visits. During the spring deployment, declining water levels required the outlet sensor to be repositioned to maintain submergence. At the inlet, the guide tube remained submerged and free of sediment blockage throughout the period, so no adjustment was necessary during the study.

The instrument recorded the following water quality parameters at 15-minute intervals:

- Water temperature (thermistor) [°C]
- pH (glass electrode with reference system) [-]
- Electrical conductivity (four-electrode conductivity cell) [µS/cm]
- Dissolved oxygen (optical luminescence sensor) [mg/l]
- Turbidity (optical nephelometric sensor, Formazin Nephelometric Units [FNU])
- fDOM (fluorescence sensor, Quinine Sulfate Units [QSU])
- Nitrate (UV nitrate sensor) [mg/l]

An integrated mechanical wiper periodically cleaned the optical windows to minimize sensor fouling and maintain data quality.

Figure 3 - Deployment Setup for EXO2 sensor Wetland Outlet (left) and Sensor deployment (software and sensor) (right, Source: Emma Lannergård, 2026)

3.5 Data processing

3.5.1 Data Quality Assurance / Quality Control (QA/QC)

HF sensor data were first quality-controlled using SentemQC, an open-source Python tool for automated QA/QC of HF water quality time series (van’t Veen et al., 2025). SentemQC is designed for high-frequency proxy sensor data and provides a harmonised and reproducible cleaning procedure across variables and events (van't Veen et al., 2025).

SentemQC anomaly detection

SentemQC identifies anomalies with moving-window filters that compare each data point with local statistics in neighbouring windows (mean, median, standard deviation and rate of change) (van’t Veen et al., 2025). Window sizes and thresholds were adopted from van't Veen et al. (2025), whose dataset included comparable proxy variables such as turbidity and nitrate. As the fDOM was not measured in the reference study, the same window properties as for turbidity were used as these 2 proxies correlate strongly. Points that exceeded these thresholds were flagged differently according to the windowsize used as potential anomalies. That way both isolated spikes and clusters of suspicious values could be detected (van’t Veen et al., 2025).

SentemQC is suppposted to be used as the first step in a broader QA/QC workflow and does not replace subsequent calibration and gap-filling required for concentration and load estimation (van’t Veen et al., 2025). All variables were analysed in the 15min interval and as hourly average. Then results from this analysis were screened manually to remove obvious spikes, sensor stabilisation periods from water chemistry, and intervals affected by maintenance or air exposure before further processing (see Appendix, figure 10 and 11). Flagged peaks where deemed plausible and were further included in the data processing.

3.5.2 Sensor units and alignment

HF fDOM and turbidity data from the EXO2 sondes were exported in manufacturer-calibrated units (QSU for fDOM, FNU for turbidity). Factory temperature corrections were retained, and no additional temperature correction was applied.

To verify HF sensor reliability and derive continuous concentrations, turbidity and fDOM were calibrated against laboratory analyses of grab samples. Grab samples were taken as close as possible to the corresponding sensor timestamps to ensure good temporal alignment between in situ measurements and laboratory analyses.
These pairs were used for site-specific regressions that underpin the conversion from HF sensor output to concentration time series (e.g. Hoffmeister et al., 2020).

Turbidity–TP calibration

Turbidity was measured with the EXO2 optical backscatter sensor (side scatter at 90 with a near-infrared LED at 860 nm) and recorded in FNU according to the manufacturer's calibration (YSI, 2012). The same turbidity channel was used in the stir-up experiment for fDOM correction and for subsequent P-proxy calculations.

To relate turbidity to P, turbidity data and TP from grab samples were paired at inlet and outlet. A paired t-test was performed to estimate whether the mean difference between the two paired turbidity measurements of the in situ measurement and the lab measurement in the population is non-zero
the TP was chosen as the response variable rather than PP because TP is the standard metric in water-quality monitoring and management. Additionally, turbidity–TP relationships commonly used to derive continuous TP estimates and loads (Lannergård et al., 2019; Villa et al., 2019). PP in this study was obtained as the difference between TP and dissolved forms, which makes it more sensitive to analytical details such as filtering procedures, whereas TP is measured directly and therefore provides a more robust basis for proxy calibration. Samples covered a range of flow conditions, with emphasis on high-flow periods when suspended sediment and particle-bound P are expected to dominate transport (Jones et al., 2011). Turbidity was used as predictor and TP as response in simple linear regressions, following established proxy approaches in agricultural catchments and rivers (Lannergård et al., 2019).

Because the same sensor type and configuration were used at both locations, turbidity–P relationships were first inspected separately (Appendix, figure 13 and

14) and then combined into a single regression when no systematic differences in slope or intercept were evident. This combined calibration was applied to the HF turbidity time series to estimate continuous TP concentrations at inlet and outlet. They were then combined with discharge data to calculate P loads and P retention in the wetland.

fDOM–DOC calibration

The fDOM signal was measured with an EXO2 fluorescence sensor (excitation 365 nm, emission 480 nm), which detects the fluorescence emission of coloured dissolved organic matter, and was recorded in QSU (YSI, 2012). The Unit [QSU] was used for the turbidity stir-up test, all turbidity corrections (fDOM_corr) and the DOC calibration.

To correct for turbidity interference, a field experiment like Hoffmeister et al. (2020) was carried out. Sediment around the sensor was manually stirred to generate elevated turbidity, while DOC was assumed constant over the short test period (Hoffmeister et al., 2020). During the subsequent decay of turbidity, paired turbidity and fDOM values were recorded and used to derive an empirical attenuation function. This function was applied to the full fDOM time series to obtain fDOM_corr, and the correction was only used within the turbidity range covered during the experiment (Hoffmeister et al., 2020).

At the inlet, coarser sediment produced only moderate turbidity during the stir-up test, so the correction there is less well constrained and may under-correct very high event turbidity. Attempts to correct inner-filter effects with an absorbance-based method following Hoffmeister et al. (2020) were not successful and were not used in the final processing.

Turbidity-corrected fDOM from inlet and outlet was paired with DOC conc. from grab samples. A single linear regression with fDOM_corr as predictor and DOC as response was fitted and used as a site-specific fDOM–DOC transfer function, following DOC proxy approaches (Hoffmeister et al., 2020). This function was applied to the corrected fDOM time series to generate continuous DOC concentrations and DOC loads at inlet and outlet.

Nitrate sensor calibration

Nitrate was measured with the EXO NitraLED UV absorbance sensor (235 nm and 275 nm), which uses a dual-wavelength design to measure nitrate absorbance while correcting for natural organic matter interference, recorded in mg/l NO_3-N (YSI, 2012).

For nitrate, the EXO NitraLED sensor was initially calibrated in the laboratory with water samples collected from the site following the manufacturer's procedures to account for site-specific influences such as turbidity and natural organic matter (YSI, 2012). Although sensor readings appeared internally consistent immediately after calibration, redeployment revealed repeated and variable offsets relative to lab nitrate. That indicated unstable performance over short time scales. These offsets would introduce substantial uncertainty into nitrate and loads which is why the NitraLED data were deemed unreliable before applying SentemQC and the following analysis. All nitrate estimates and subsequent N calculations based on the NitraLED sensor were excluded from the process due to the offset (Appendix, figure 12).

3.5.3 Calculations

For the load calculations in this thesis, it was explicitly looked at certain events instead of the whole survey time. This allowed to check for more detailed information such as τ_{th}, water packages, hysteresis effects and sediment mobilisation threshold.

Event definition

To account for the time delay caused by wetland buffering, loads and retention were analysed at the event scale. Only distinct flow events were considered, because baseflow contributions were inconsistent during the measurement period and could not be characterised reliably.

Operational event criteria

Events were derived from the inflow and outflow discharge record, because no local on-site precipitation data was available. The available rainfall data from the nearest weather station did not consistently reproduce the on-site flow increase and were therefore unsuitable as a primary event indicator. Additionally, Precipitation events alone could not be used as initiation conditions due to snow formation, which made the rain amount an unsuitable proxy for this study. An event was defined as starting equation (IX) when inflow discharge rose sharply compared with the previous timestep, i.e. when flow began to increase from assumed baseline levels.

As no consistent baseline level could be determined an event was assumed to end (equation X) when outflow discharge sank to a local minimum after the peak before increasing again due to a following event.

Equation IX

$$Q_t[\frac{m^3}{h}] > 1.5 \times Q_{t-1}[\frac{m^3}{h}]$$

$$Q_t[\frac{m^3}{h}] < Q_{t-1}[\frac{m^3}{h}] \text{ and } Q_t[\frac{m^3}{h}] < Q_{t+1}[\frac{m^3}{h}] \qquad \textit{Equation X}$$

This procedure allowed overlapping events to be separated, accepting that residual contributions from preceding or following events may be neglected.

With this definition, an event ends at a local minimum in outflow discharge. Where no such minimum was clearly identifiable because discharge declined only asymptotically over a long period, the event end was defined manually. One event was completely identified manually, because it was initiated by snowmelt and the centroid method with a 50% increase in inflow rate as trigger was not applicable.

Theoretical water residence time

The effective wetland volume V_{eff} was estimated from bathymetry mean water levels measurements, recorded at the end of the monitoring period. For each hourly HF timestep, hourly τ_{th} was calculated (equation IV). To obtain a single representative τ_{th} value per event, a discharge-weighted mean was calculated using equation VI with t being the instantaneous $\tau_{\text{th}}(t)$, weighting each hourly $\tau_{\text{th}}$by the corresponding inflow discharge. This approach ensures that timesteps with high discharge — which are hydraulically most relevant — contribute more strongly to the event mean than low-flow periods.

The effective water surface area of the wetland was first delineated and measured using high-resolution aerial imagery in Google Earth. The wetland was then subdivided into a deep inlet basin and a downstream shallow area with emergent vegetation, following the general design described by Kynkäänniemi (2014). In this study, the shallow downstream area was subdivided into four zones, representing the 4 in series connected pools of the shallow part of the wetland. Those zones were of approximately equal size. This deviation was used to capture internal variation in depth and hydraulics. For each zone, mean water depth was calculated from five randomly distributed measurements at the 28th of April 2026 around 11am. These depths were multiplied by the corresponding surface area, and the effective water volume of the shallow area was obtained as the sum of these four sub-volumes.

Centroid-based Q-lag and conc.-lag

Because HF discharge was measured at both inlet and outlet, event-scale travel times were additionally quantified using centroid-based lags. For each event, flow-weighted centroids were calculated as described in equation VI and VII to account for hydraulic delay. The lag for each event was then defined as in equation VIII. Analogous centroids were computed for flow-weighted concentrations to obtain a conc.-lag for each event (equation VI, VII and VIII). They were used to evaluate concentration changes along the flow path related to mobilisation processes, such as sediment remobilisation during rising limbs. Where TP and DOC conc.-lags did not differ systematically, the same lag was applied to both constituents to keep the analysis consistent. These Q- and conc.-lags were used to align inflow and outflow "water packages". To achieve this the Inflow data were shifted to align with the Outflow data in the mass balance. τ_{th} served only as a comparative hydraulic indicator (equation XI and XII).

$$Q_{in,\,shifted}(t)[\frac{\mathrm{m}^3}{\mathrm{h}}] = Q_{in}(t - Lag)[\frac{\mathrm{m}^3}{\mathrm{h}}]$$ *Equation XI*

$$conc_{in,\,shifted}(t)[\frac{g}{m^3}] = conc_{in}(t - Lag)[\frac{g}{m^3}]$$ *Equation XII*

Inflow-outflow event mass balance calculations

For each event hour, inflowing and outflowing mass (g/h) was estimated for an event with equation I. TP concentrations were derived from turbidity using the site-specific turbidity–TP regression in Figure 5, and DOC concentrations from fDOM using the regression in Figure 7. Hourly retentions (equation. I) were summed to calculate the total event load.

Critical discharge and retention

To identify thresholds for sediment and TP mobilisation, hourly retention was related to the time-shifted inflow discharge using the Q-lag-corrected hydrograph on an event scale. A critical discharge for mobilisation was defined as the point where retention shifted from net retention to net export.

Event hysteresis analysis

For hysteresis analysis, the same event boundaries as in the load and retention calculations were used. Within each event, concentration–discharge (C–Q) pairs were generated by linking unshifted concentrations with the corresponding unshifted discharge at each hourly HF timestep. These C–Q trajectories were used to examine event-scale hysteresis patterns for TP and DOC (Lannergård et al., 2021).

4. Results

4.1 Evaluation of C and P proxies

This section evaluated whether the high-frequency sensor signals could be used as proxies for TP and DOC, which addressed research question 1. First, the turbidity–TP relationship was assessed, followed by the fDOM–DOC calibration.

The turbidity calibration (Figure 4) showed a strong positive linear relationship ($R^2 = 0.72$, $n = 9$) between HF turbidity readings and turbidity from grab samples. A paired t-test confirmed no statistically significant difference between the two measurement series ($t = 0.814$, $p = 0.439$, $n = 9$). Overall, the HF turbidity sensor performed reliably across the measured range, though some scatter at intermediate concentrations suggests limited precision under those conditions.

After, the turbidity data from the grab samples were plotted against the TP concentration from the grab samples, taken at the same timestep (Figure 5). This showed a strong linear relationship (R^2=0.93, n=13) between turbidity and TP concentrations allowing the fitted equation to be applied to the HF turbidity time series to derive continuous TP conc.

The stir-up experiment needed for the turbidity correction for the DOC measurement revealed a clear negative relationship (R^2=0.79, n=72) between fDOM sensor measurement and turbidity concentrations in the water (Figure 6). This confirmed that increasing turbidity systematically attenuated the fluorescence signal and justified the use of a turbidity-based correction function for fDOM before DOC calibration.

The fDOM–DOC correlation showed a weak positive linear trend (Figure 7), with considerable scatter and a lower coefficient of determination (R^2=0.23, n=15). The use of this as a proxy was applied initially with the thought that the data might not be representable for the data analysis.

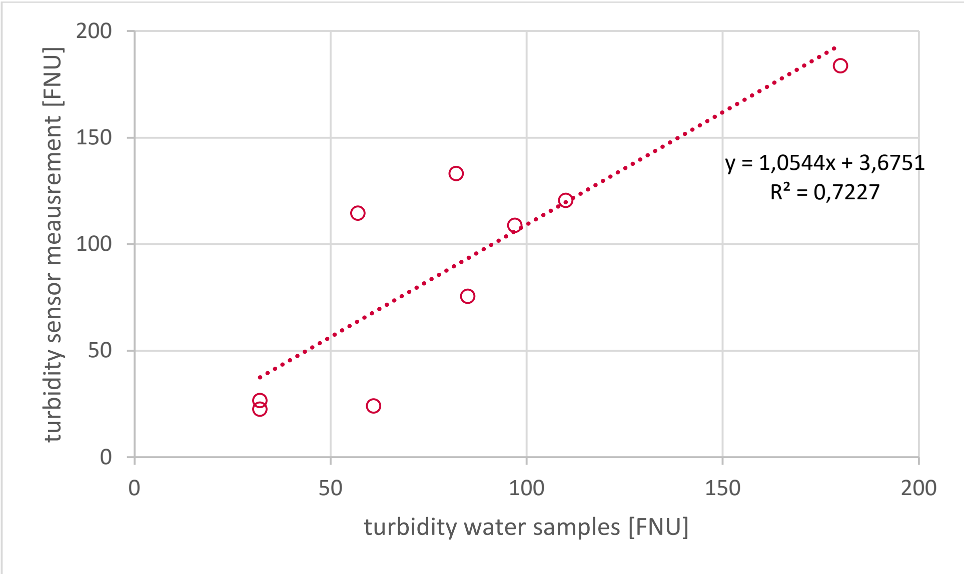

Figure 4 - Correlation between turbidity [FNU] in water samples and measurements with turbidity sensor [FNU] (n=9). Observations are indicated by the red dots and regression line (red dotted).

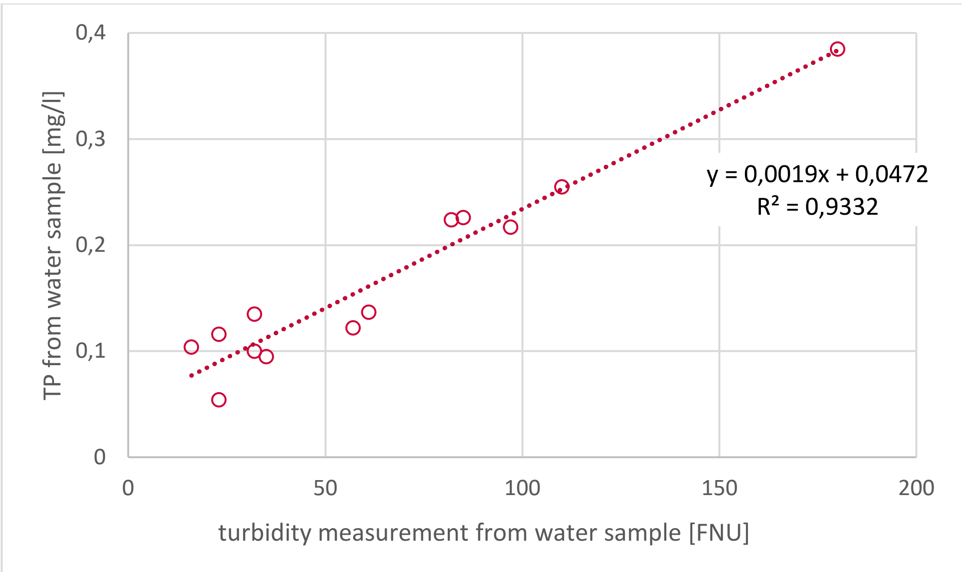

Figure 5 - Calibration of turbidity (FNU) against TP (n=13). Observations are indicated by the red dots and regression line (red dotted).

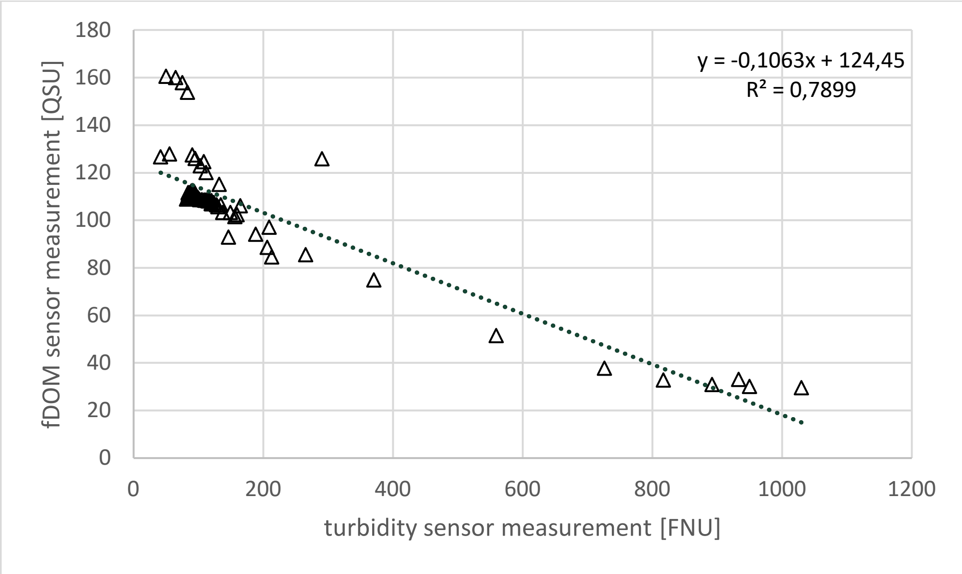

Figure 6 - Relationship between fDOM (QSU) on y-axis and Turbidity (FNU) on x-axis (n=72). Observations are indicated by the black trinagle and regression line (black dotted).

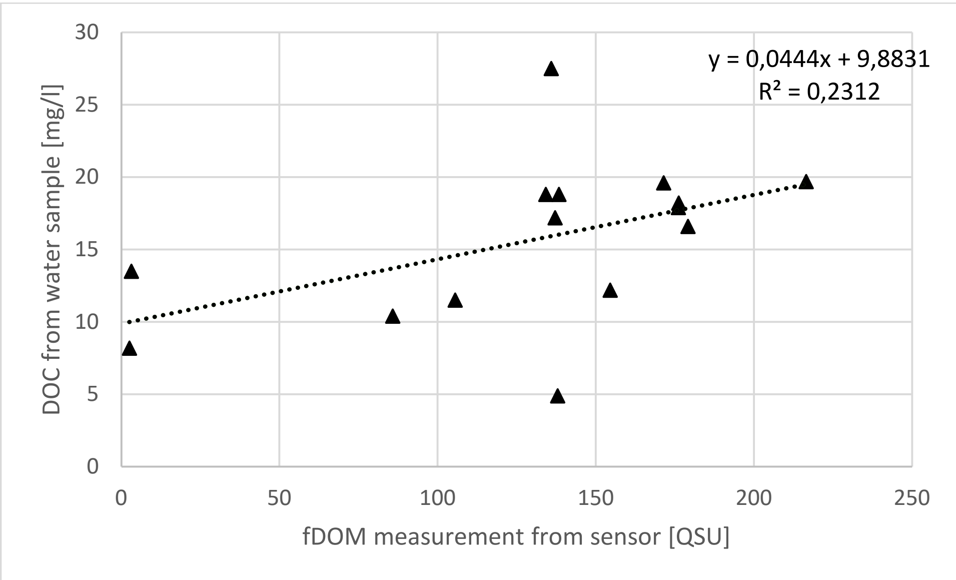

Figure 7 - fDOM–DOC relationship for DOC estimation (n=15). Observations are indicated by the black triangle and regression line (black dotted).

Through the fit of the regression between the water samples and the HF sensor measurements, the equation could be applied to the continuous measurements of the HF data, allowing to calculate the concentrations of TP and DOC on an hourly basis according to our measurements shown in Figure 8 below.

4.2 Discharge and water quality

In this part of the results the general correlation of turbidity-TP and fDOM-DOC was applied to the HF data, to get the continuous high-frequency estimates of TP and DOC concentrations at the inlet and outlet.

4.2.1 Hydrology and event timing

Snow depth increased from early December to late March, with several melt and rainfall episodes superimposed on the snowpack (Figure 8a). The discharge time series shows six high-flow periods: four early-winter events during the first deployment and two longer spring events following snowmelt and precipitation (Figure 8b). For all events, outlet discharge curves were smoother and slightly delayed relative to inlet discharge, indicating hydrological buffering of short-term peaks within the wetland.

4.2.2 Turbidity and TP concentrations

Turbidity values and TP conc. at the inlet exhibited pronounced peaks during the early-winter and spring events, reaching values above 600 FNU or 1 mg/L during the main spring peak (Figure 8c). Outlet TP conc. generally followed the temporal pattern of the inlet but with slightly damped peaks. During lower-flow periods between events, TP remained at comparatively low and stable levels at both inlet and outlet.

4.2.3 DOC concentrations

DOC conc. showed similar event-scale variability to TP (Figure 8d). fDOM reacted opposite to turbidity. Maximum fDOM values were in the reach of 230 QSU, equal to a DOC conc. of approximately 20mg/l. Outlet DOC conc. were consistently more different to the Inlet data than for TP. No clear lag between inlet and outlet DOC signals is apparent at the daily scale.
A pronounced drop in DOC in the outlet occurred between 21.3.2026 and 31.3.2026, it is not possible to infer the reason for this behaviour from other sensor observation or weather data.

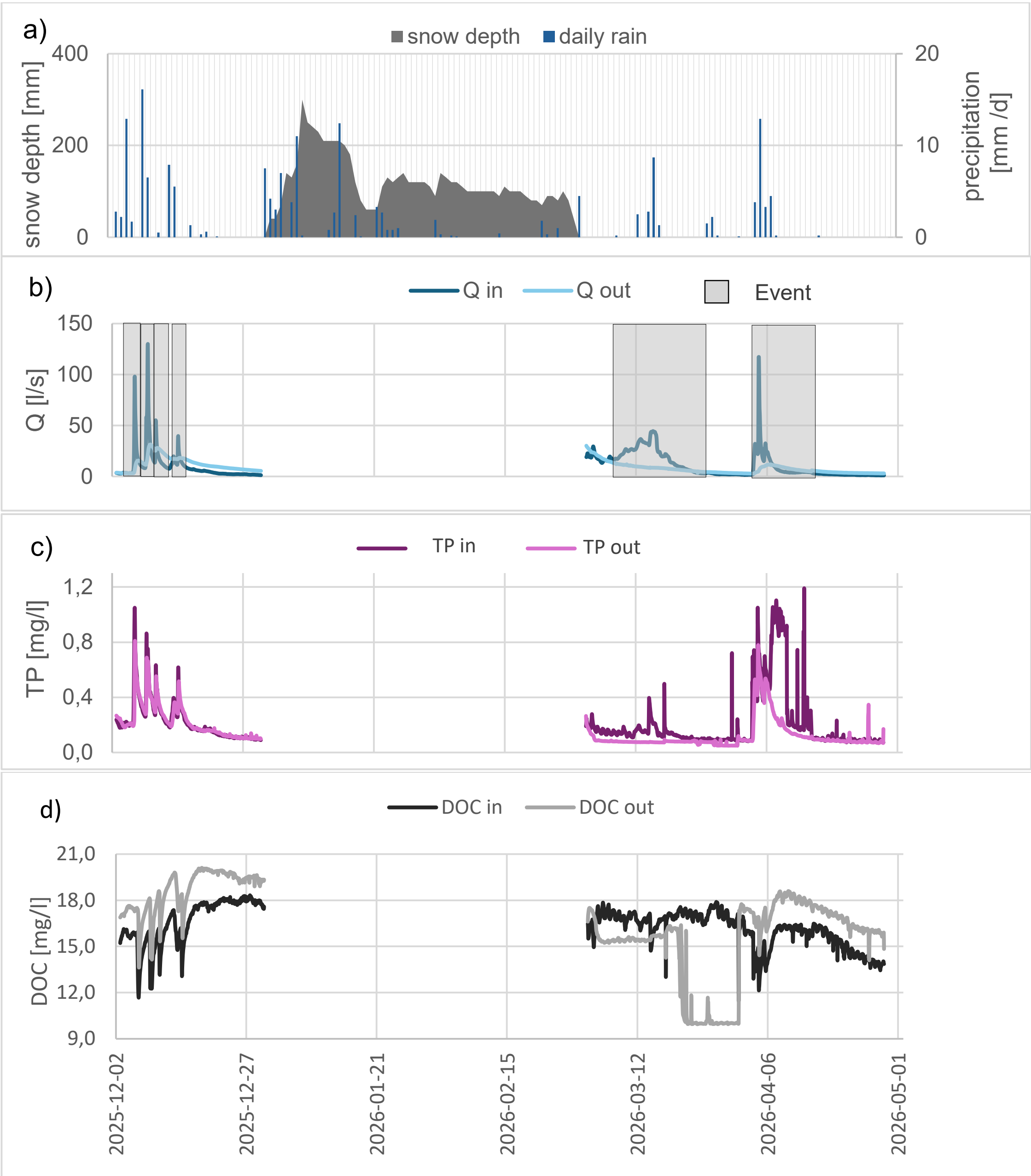

Figure 8 - Flow and concentration curves during sensor deployment a) precipitation [mm/d] in blue bars, snow depth [mm] in grey; b) Events in grey boxes, Flow[l/s] for inlet (dark blue] and outlet (light blue); c) Total phosphorus concentration [mg/l] for inlet (dark violet) and outlet (light violet); d) dissolved organic carbon concentration [mg/l] for inlet (black) and outlet (grey)

4.2.4 Hydrological events

Application of the event-definition procedure resulted in six events during the study period (Figure 8b). Events 1–3 in early December were identified using the 50% discharge-increase criterion and lasted approximately 54 h, 43 h, and 82 h, respectively. Event 4 marks the final early-winter peak in discharge and extended over about 380 h, with an alternative, shorter definition ending after roughly 100 h also considered as the outflow still changed asymptotically. Event 5 corresponds to the main spring snowmelt period and had a duration of about 530 h, while event 6 captures a subsequent April rainfall-driven peak lasting around 270 h. An alternative, shorter definition ending after roughly 92 h was also considered. For event 5, the start and end were selected manually because discharge did not trigger the defined threshold, whereas event starts 1–4 and 6 were identified directly by the 50% criterion applied to the inlet discharge time series. For the ongoing analysis the alternative event end for Events 4 and 6 were used.

4.2.5 Hydraulic lag and theoretical residence time

Centroid-based lags between inlet and outlet discharge ranged from 7.6 to 15.9 h for events 1–4 and 6, indicating flow translation through the wetland on sub-daily to roughly half-day timescales (Table 1). Event 5 represented the main snowmelt period and was the only one, with a negative centroid lag (−40.6 h). This showed that applying these boundaries, the outlet centroid occurred earlier than the inlet centroid within the chosen event window and that the selected centroid did not cover the water package.

τ_{th}, was calculated from a stagnant V_{eff} during the end of the monitoring period and event-averaged inlet discharge. It ranged with similar behaviour but overall shorter retention times from 3.4 to 12.9 h. For the Load calculation all lag values were rounded to full hourly values to shift to the hourly measurements correctly.

4.2.6 TP retention

Overall hydraulic load–retention relationships across events

Event-wise analysis of the HL–retention relationships revealed that all six events shared a broadly similar pattern. The range over which the sensors operated, differed in the magnitude of retention and the HL (Figure 9). Three events - 1, 2, and 6 - followed particularly similar patterns: retention started from near-zero or slightly negative values at low HL (smaller than 0.1 m/h) and then increased almost linearly with hydraulic loading, reaching clearly positive values at moderate (between 0.1 and 0.15 m/h) to high HL (above 0.15 m/h). No pronounced decline at the upper end of the observed HL range was detected. In contrast, Event 3, 4, and the snowmelt event (5) showed comparable responses at below 0.1 m/h retention levels. These events showed lower maximum HL and retention in the HL–retention relationship (Appendix, figures 14-19).

Across all six events, the HL–retention plots (Figure 9) showed a coherent pattern:

- At low HL (typically about 0.05–0.1 m/h), hourly TP retention was small and in several events negative, which suggested that under these low-flow conditions the wetland could exhibit net P release.
- With increased HL, retention rose systematically in every event. Positive TP retention generally became dominant above about 0.1–0.15 m/h, and event-specific maxima ranged from 40 g/h up to more than 300 g/h TP retention at the highest HL values.
- Within the HL range observed, most events did not show a clear decline in TP retention at the higher HL, so a consistent decreasing limb was absent.

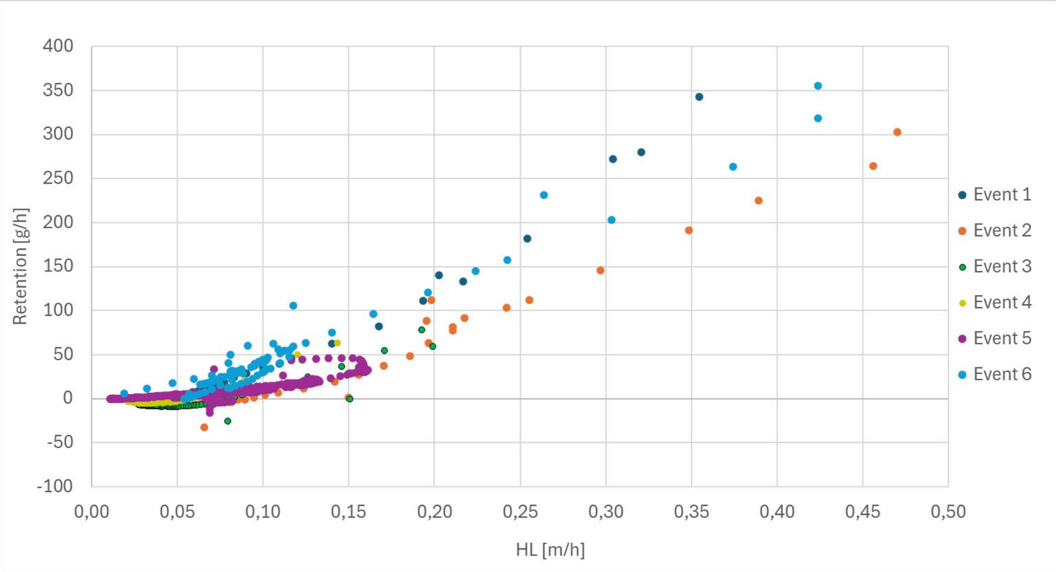

Figure 9 - Event specific phosphorus retention curves. Event 1 (dark blue), Event 2 (orange), Event 3 (green), Event 4 (yellow), Event 5 (violet), Event 6(bright blue)

4.2.7 Mass dynamics

TP and DOC concentration lags were small and clearly shorter than the corresponding hydraulic lags as shown in table 1. For TP, centroid-based lags were mostly within ±3h; events 1–4 showed outlet peaks between about 0.2 and 2.7h after the inlet peak, while Event 5 (snowmelt) estimated a similar concentration lag and Event 6 a negative lag of -1.5 h. DOC lags were of similar magnitude but consistently negative, which indicated slightly earlier DOC centroids at the outlet than at the inlet across events showing the limitations of this lag approach.

4.2.8 Retention per event

Event-scale retention was evaluated using inlet and outlet load estimates that already account for the calculated hydraulic lag between inflow and outflow. Across the six analysed events (Table 1), the wetland showed positive TP retention in four cases, with particularly high retained masses during Events 5 and 6 also due to the longer period of these Events. In contrast, Events 3 and 4 exhibited net TP export. This behaviour indicated that the wetland temporarily functioned as a TP source under the conditions present during the defined events. C retention was bigger but stayed proportionally similar except event 5 where much more C was retained.

Table 1 – Description of events, hydraulic lag, mass lag and retention.

	HYDRAULIC LAG		**MASS LAG**		**EVENT RETENTION**		
	Observed Residence Time (Centroid)	theoretical WRT	TP-conc.	DOC-conc.	TP - retention	DOC - retention	HL average
	lag [h]	lag [h]	lag [h]	lag [h]	[kg/event]	[kg/event]	[m/h]
EVENT 1	12.5	4.1	2.78	-1.35	6.72	16.71	0.12
EVENT 2	8.6	3.4	1.21	-0.79	6.97	10.46	0.13
EVENT 3	6.5	8.7	-0.59	-0.09	-0.74	-52.02	0.05
EVENT 4	10,3	12.9	0.63	-0.72	-0.37	-45.32	0.04
EVENT 5	-40.6	6.8	0.25	-41.36	15.16	30.63	0.07
EVENT 6	15.9	4.9	-1.53	-0.96	14.15	78.61	0.09

4.2.9 Hysteresis

Hysteresis loops for TP concentration versus discharge were plotted for both inlet and outlet across all six events (Appendix, figures 21 and 22). At the inlet, events 1–4 and 6 showed clear clockwise or counterclockwise loops (Table 2). That indicated differences in concentration during the rising and falling limbs of the hydrograph. Event 5 exhibited a much more scattered and complex pattern (Appendix, figures 22), with multiple overlapping concentration–discharge trajectories. No simple closed loop was detected, making systematic hysteresis characterisation difficult for this snowmelt event.

At the outlet, hysteresis patterns were generally present but with less pronounced loop closure than at the inlet in several events. This shows a more delayed response at the outlet and more variability in the conc. - Q relationship. Events 1-4, and 6 showed relatively clear clockwise loops showing an increase in TP conc. before a maximum Q is met. Event 5 again showed no interpretable single loop structure.

Event 3 and 4 differed from the previous events, with counterclockwise hysteresis at the inlet and clockwise hysteresis at the outlet (Table 2). Event 4 closely resembled event 3, with a similar inlet pattern and a clockwise outlet hysteresis that was also very similar in shape.

Overall, the results suggest that the outlet response was more consistently clockwise, while the inlet showed greater event-to-event variability.

DOC–discharge hysteresis was not analysed because DOC concentrations showed minimal event-scale variability and the fDOM–DOC proxy had limited predictive power ($R^2 = 0.23$), making hysteresis patterns uninformative for the objectives of this study.

Table 2 - Hysteresis patterns for each event inlet/outlet.

	INLET	OUTLET
EVENT 1	**clockwise /linear**	**clockwise**
EVENT 2	**clockwise /linear**	**clockwise**
EVENT 3	**Counterclockwise**	**clockwise**
EVENT 4	**Counterclockwise**	**clockwise**
EVENT 5	**-**	**-**
EVENT 6	**Clockwise**	**clockwise**

5. Discussion

5.1 High-frequency proxies for TP, DOC and Nitrate

Measurements for monitoring TP had a strong relationship between the parameters in Nybble. Grab samples showed a strong linear relationship (R^2 = 0.93, n = 13) between turbidity and TP.
Although the sampling size was not large, it was possible to cover turbidty values with only 10s of FNU up to 600 FNU during the research period from 14th November 2025 until the 28th of April 2026. With this consideration the turbidity was a good fit for the TP estimation. This allowed efficient usage of the HF data measurements as a robust surrogate for TP in this wetland. The study period turbidity measurements (Figure 4) covered a wide range of flow conditions and suggests that the HF sensor tracked grab-sample turbidity well (R^2 = 0.73, n = 9) during the deployment period. As the calculations estimations of TP rely on a relationship derived from lab data, the difference between the labratory turbidity measurements and the HF sensor turbidity measurements can cause a difference in estimations of TP.

This data supported the previous studies, suggesting using optical HF measurements for TP load estimates in dynamic systems (Lannergård, 2016). For particle-dominated P transport, turbidity-based monitoring can therefore provide the temporal resolution needed to capture short-lived concentration peaks during short high flow events (Bieroza et al., 2023).

In contrast, the fDOM–DOC proxy showed much weaker predictive performance (R^2 = 0.23), so fDOM alone explained only a limited fraction of DOC variability at Nybble.
DOC varies with hydrological conditions, catchment sources and in-stream biogeochemical processes, and optical DOC measurements require corrections for matrix effects such as inner filter effects, as shown by Hoffmeister et al. (2020). Although the suggested temperature and turbidity correction was successful, the correction for the inner filter effects might improve the performance of the fDOM-DOC proxy in future studies.

For the first deployment period Nitrate was only measured at the outlet due to the availability of functioning NitraLED sensors. Comparison of the data was not possible during that research period.
The site-specific nitrate calibration for the sensor was applied prior each deployment. Following the deployment, values became negative, indicating clear limitations in the reliability of the sensor data. As negative readings are physically implausible in this context, the nitrate data were not further analysed. In concept, a negative conc. would imply that the detected output signal exceeded the emitted input signal of the sensor after correction. Signal drift or unaccounted

interferences in the optical path might be issues which could not be further investigated due to time limitations.

5.2 Hydraulic loading and P retention

High frequency monitoring enabled detailed analysis regarding retention behaviour during different flow conditions.

Although the HL–retention plots differed for each event, similarities could be observed. Under HL lesser than 0.1m/h, a negative retention could be observed. Additionally, the overall trend of the plots showed a TP retention increase from low to our maximum covered HL.

A threshold of approximately 0.1 m/h was identified, above which event-scale TP retention occurred. At HL below 0.1 m/h, in those event boundaries the wetland sometimes acted as a TP source, reflecting remobilisation of previously accumulated TP. Over the period when optical sensors were deployed, the average HL was about 0.038 m/h, which would correspond to an annual HL of roughly 300–350 m/year if such conditions were sustained throughout the year. However, this average mainly reflects monitored high-flow periods and does not include low-flow summer conditions.

Inflows exceeding the 0.1 m/h threshold (27.8 l/s for a wetland area of 1000 m²) occurred exclusively during covered events rather than representing typical year-round conditions. This threshold (equalling 876 m/year) covered short-term behaviour in a system with substantial internal TP stores and differs fundamentally from the annual HL threshold of about 300 - 400 m/year reported by Kynkäänniemi (2014). This study from 2014 was based on long-term inflow–outflow balances and sediment sampling where no optical sensors where used. There the findings showed that the annual P accumulation on sediment plates decreased at high HL in small P-wetlands on agricultural clay soils.

During the conditions observed, increasing event-scale HL increased the estimated TP retention. Earlier work by Kynkäänniemi (2014) reported that annual P accumulation decline at much lower annual HL (300–400 m/year) in similar settings. This apparent difference can be explained by the variations in time scale, system state and hydrological regimes of those studies.

The 0.1 m/h threshold identified, described short-term event behaviour in a wetland in which internal TP accumulated over time. The threshold reported by Kynkäänniemi (2014) reflects long-term annual HL. When this average HL was reached, sediment accumulation decreased in small P-wetlands due to frequent high-flow conditions. In other words, the present event-based optical-sensor analysis showed how the wetland functions during individual high flow events, while the earlier studies showed annual scale mass-balance and how repeated high loads over entire years affect TP storage. The thresholds from these two approaches have to be seen as complementary perspectives on wetland functioning rather than as directly comparable or contradictory values.

Land et al. (2016) showed in a broad systematic review of 203 wetlands that TP removal efficiency decreases from around 60% TP retention with a constant HL to around 21 % in wetlands with precipitation-driven compared to controlled hydraulic regimes. This shows the impact of changing HL in the system further showing the importance of understanding event driven behaviour and the need for further research.

This event driven Retention gives further insight for future work needed to understand wetland behaviour. With the event analysis and the following definition, a threshold could be estimated which could be used to limit conditions which favour TP release.

High hydraulic loading rates and short-circuiting reduce hydraulic efficiency and effective treatment volume in constructed wetlands (Persson et al., 1999), and cold-climate studies show that concentrated flow paths can further limit contact between water and wetland media (Smith et al., 2005).

As Kynkäänniemi (2014) mentions, Nybble is with only 0.13% on the smaller end of recommended wetland sizes. Increasing the relative wetland area, lengthening flow paths (e.g. meanders or multi-cell layouts), and using upstream detention to attenuate inflow peaks are all measures that can reduce effective HL at the wetland inlet and improve hydraulic efficiency (Persson et al., 1999; Kadlec and Wallace, 2009). This could help increase the retention function of the wetland.

Further management procedures to ensure the best possible TP retention include Periodic removal of accumulated fine sediment (Mendes, 2020) and managing vegetation by promoting deposition and stabilizing wetland conditions (Braskerud, 2002).

5.3 Inlet–outlet patterns

Through high-frequency monitoring both in the inlet and outlet of the wetland it was possible to analyse processes connected to concentrations and discharge in the wetland during the study period.

During high-flow events, inflow TP concentrations showed sharp peaks likely linked to runoff from the upstream fields. Outlet peaks were smaller and only slightly delayed, indicating retention of particle-bound P as water passed through the wetland with turbidity peak values being reduced up to 20% (Event 1).

In this context it is also crucial to mention, that events partially influenced the following event conditions. If the events instantly followed one another like in Event 1 - 4 the Outflow is already increased and might be corresponding differently as when no event was immediately before. In between the defined events, Inflow and Outflow TP concentrations were much more similar, and several periods showed enrichment at the outlet, which may indicate remobilisation of previously deposited phosphorus from wetland sediments under low-flow conditions.

These findings agree with Mendes, (2020) who demonstrated that older surface-flow constructed wetlands with high P saturation or low incoming P loads can show P release. This is because of the saturation of Fe- and Al-oxide sorption sites, the reducing conditions at the sediment–water interface releasing the Fe-bound P, and low inflow P concentrations favouring desorption across the soil–water interface.

One option to confirm this assumption would be further lab analysis of the sediment and investigations on dissolved oxygen and pH conditions, which where out of the scope of this thesis.

DOC showed only modest event-scale variability and inlet–outlet differences, so DOC contrasts were much less pronounced than for TP. Additionally, it was observed that the DOC concentration at the Outlet was for most of the research period higher than at the inlet.

Together, these patterns indicate that the wetland functioned mainly as a TP and DOC sink during event flows but could act as a temporary internal source during extended low-flow periods when external inputs were small and internal processes dominate.

5.4 Hydraulic and concentration lags

The use of the centroid method proved effective for simple precipitation event analysis, although certain restrictions must be made. For events 1–4 and 6, Q-lags ranged from about 6.5 h to 15.9 h, which implied sub-daily to roughly half-day travel times for event water through the wetland.

These values ranged between 0.8 and 3 times the amount of the τ_{th}. Event 3 and 4 (Table 1) were the events where the τ_{th} had a longer residence time then the centroid method, although that result is likely caused by the low flow, as these events had the lowest peaks of all events and lowest averaged HL. This might affect the τ_{th} as it was calculated by a fixed water table, overestimating the residence time.

The data of this model, which added outflow estimates suggest one of two things. During the defined events, the use of a fixed V_{eff} during the whole period was insufficient for this kind of comparison and water high measurement at Nybble should be implemented for further research.

Alternatively, τ_{th} (based on volume and flow) can overestimate how long water actually interacts with the wetland. Stagnant or poorly connected storage areas create dead zones and preferential flow paths, causing much of the water being bypassed these volumes and having a shorter contact time. Observations during low-flow conditions, stagnant areas were clearly visible, supporting the idea of inactive volumes.

In contrast, event 5 (snowmelt) showed a large negative lag, which suggests that the manually defined event window did not isolate a single hydrograph "water package" sufficiently. The high negative lag implies that the outflow data did not correspond to the inflow data, and the centroid approach does not apply for proper event definition in this case. Future work in mixed-regime catchments will need more flexible, multi-criteria event definitions or separate treatment of snowmelt and rainfall events for better event definition.

TP concentration lags were small, mostly within ±3 h, and substantially shorter than the corresponding Q-lags and WRT, indicating a faster TP mobilisation than expected from throughflow alone. This decoupling suggests that internal processes, such as mobilisation of stored sediment and biomass-bound P, contribute to outlet TP dynamics. These findings could agree with studies showing that wetlands can intermittently release stored P under specific conditions. Jarvie et al. (2020) showed that during low-flow, high microbial activity and redox changes can mobilise legacy P from sediments. The study refers to warm summer conditions so further research would be necessary to sufficiently analyse the situation for low flow winter and spring conditions. Mendes (2020) reported P release from older constructed wetlands when P sorption sites are saturated or inflow concentrations are low which would need further investigation on water chemistry during these low flow conditions which were not in the scope of this study.

5.5 Hysteresis and event timing

Through analysis of hysteresis patterns, mobilisation processes could be examined during the identified events.

At the inlet, events 1, 2, and 6 showed clockwise or near-linear conc. - Q patterns. This could be explained by rapid mobilisation of nearby particulate sources on the rising limb and dilution on the falling limb (Lloyd et al., 2016; Moatar et al., 2017). Events 3 and 4 showed counterclockwise hysteresis at the inlet, indicating that concentration peaks occurred later than discharge peaks and suggesting delayed source contributions, potentially via more distal source areas (Vaughan et al., 2017). At the outlet, hysteresis was more consistently clockwise across events 1–4 and 6, which points to rapid mobilisation of internal P sources early in the hydrograph (Ulén et al., 2019).

Events 3 and 4 showed a shift from counterclockwise hysteresis at the inlet to clockwise hysteresis at the outlet, which may indicate internal remobilisation of previously deposited sediment P.
Notably, events 3 and 4 showed net P export and were also the events with the lowest average hydraulic loading (0.11 and 0.07 m/h respectively) and observed residence times shorter than the theoretical water residence time, further suggesting short-circuiting within the wetland during these low-flow events. For further analysis during these small HLs additional dissolved oxygen levels need to be monitored and analysed together with the data derived from this study. In addition, an uncertainty remains in the Q estimates at the outlet since groundwater contributions near the outlet or a poor hydraulic connection between the outlet pipe and surrounding sediments could bias Q measurements.

For Event 5 no pattern could be determined, as several small peaks occurred during the defined boundaries showing limitations in the method applied.

The combination of short TP conc. lags and clockwise outlet hysteresis implies that internal P-rich sediment stores respond quickly to rising flows and can influence short-term TP export, even when the wetland is a net sink at the event scale. The event boundaries and effects of preceding events on flow and storage therefore need to be considered when interpreting event-scale retention metrics and attributing individual events to external versus internal sources.

5.6 Limitations

The study was a success for implementing the turbidity-TP relationship to high frequency data. Retention calculations for simple precipitation events were applicable, not including event 5 which would need more advanced analysis for the event boundaries. Using this Event scale approach might neglect influence of previous events. Several methodological limitations must be considered when interpreting these results.

5.6.1 Study period

The study period from November 2025 to April 2026 covered late autumn, winter, and early spring but did not include summer baseflow or late-spring and early-summer rainfall events. Seasonal differences in vegetation density, temperature-dependent biogeochemical processes were therefore not fully represented, and the findings may not describe year-round wetland behaviour. Even with these limitations, the HF dataset provides a more detailed and mechanistic view of event-scale P dynamics than conventional grab sampling or proportional flow monitoring alone and shows how P retention in this small agricultural wetland is governed by non-linear, hydraulically driven processes that include both retention and remobilisation phases.

5.6.2 Sensors

SentemQC performed well in flagging obvious anomalies in the high-frequency data; however, because the underlying statistics treated extreme values as outliers, peak-flow conditions were also frequently flagged, even though these were precisely the observations of greatest interest so an automated approach in data clearing was not applicable. Consequently, careful manual review of the flagged data remained essential.

While turbidity provided a robust proxy for TP, extending HF monitoring to DOC and nitrogen will require more robust calibration and better correction for interference.

The NitraLED sensor uses a dual-wavelength design intended to improve robustness under variable DOC/NOM conditions, but this does not fully eliminate interference or long-term drift. Previous work suggests that full-spectrum UV sensors and frequent field calibration can improve nitrate measurements in similar environments (Pellerin, 2016). Where such equipment is not available, event-integrated grab-sample budgets may remain the most reliable option for nitrogen measurements.

The fDOM-DOC relationship gave an insufficient R^2 for robust usage as a proxy. The temperature and turbidity correction of the fDOM data were not enough to create a clear relationship to DOC sufficiently. This might be since it was not possible to account for inner filter effects as Hoffmeister (2020) suggests, or to the small sample size.

The weak fDOM–DOC proxy and the unstable nitrate sensor performance also highlight the suggestions made by Bieroza et al. (2023), that multi-parameter HF monitoring requires careful calibration, maintenance, and quality control to provide reliable data for water monitoring management.

5.6.3 Event boundaries and theoretical water residence time

For the event analysis of this thesis a centroid method was applied to the flow data to estimate a time lag of the water packages passing the wetland. The method was effective in determining simple events, where Inflow and Outflow water packages could be coupled. The definition of the boundaries was very simple and should be improved for future studies with for example additional on site precipitation data. The definition was insufficient to estimate all event endings, where 2 had to be defined manually. The snowmelt event was also not detected automatically showing that more sophisticated models are needed for analysing events with more complex Q pattern.

The hydraulic lag derived from the centroid method provided a good match between inflow and outflow water packages for most events, but the concentration lag was notably shorter, indicating that concentration peaks propagate through the wetland faster than the bulk water mass. As a result, outflow loads were calculated using concentrations corresponding to the Q-lag rather than the shorter conc.-lag, which may have led to a slight underestimation of outflow loads and a corresponding overestimation of retention. The influence of previous events to following ones was also not considered and might have influenced Retention functions and lag estimates as Outflow data was still partially affected from previous Inflow and not in increased due to the water packages. This might have made the lags shorter, than they would have been without previous influence.

Water depth measurements were conducted only once, at the end of the monitoring period under low-flow conditions, which introduces two distinct sources of uncertainty. First, during the measurement campaign, parts of the shallow wetland zone were dry or inactive. Although sampling locations were randomised, there is a risk that dry areas were underrepresented, leading to an overestimation of the wetland surface area and consequently V_{eff} under low-flow conditions. This would cause HL to be underestimated relative to the true active wetland area.

Second, since water depths were measured under low-flow conditions, they are not representative of the higher water levels occurring during events. V_{eff} was therefore likely underestimated during high-flow periods, resulting in τ_{th} values being underrepresented.

Continuous water level measurements throughout the monitoring period would have allowed dynamic estimates of V_{eff} and improved the accuracy of both HL and τ_{th} calculations.

Under low-flow conditions, flow concentrated into small channels in the shallow part of the wetland, creating preferential flow paths and substantially increased local HL within the channels, potentially favouring remobilisation of stored TP. These low-flow situations and critical Q causing these situations were not captured by the event-based analyses and therefore remain outside the quantitative assessment.

6. Conclusion

This study shows that HF monitoring with optical sensors provides improved process understanding of event-scale P dynamics in a small agricultural constructed wetland that cannot be achieved with conventional low-frequency sampling. The turbidity-based TP proxy performed robustly and allowed continuous estimation of TP concentrations. and loads across different flow conditions. The hydrological model for travel time and centroid lags reproduced observed timing patterns well for simple events to interpret concentration responses in relation to hydraulic forcing but underrepresenting the influence from previous events. Event 5 (snowmelt) would need further analysis because of the flow pattern caused by the snowmelt.

The Nybble wetland acted as an effective short-term TP sink under HL above 0.1 m/h during the events with increasing retention as HL rose from low to moderate values. At HL below 0.1m/h, especially periods before events, retention was often close to zero or negative, indicating that internal P sources in surface sediments can dominate when flow is small. Further analysis for these conditions is needed regarding microbiological processes. Within the hydraulic loading range covered by the monitored events, retention generally continued to increase at higher HL rather than showing a decline at a certain HL.

Short TP concentration lags relative to inflow and the predominance of clockwise hysteresis at the outlet demonstrate that internal sediment stores respond rapidly to changing discharge. The broadly consistent agreement between centroid Q-lags and τ_{th} for most events could supports the use of a simple hydrological model with an V_{eff} to describe bulk flow through the system where Outflow is not measurable. Deviations for individual events highlight the role of preferential flow and changing active volume during larger or more complex events. They may also reflect the formation of preferential flow paths during low-flow periods that are not fully captured when only discharge is available and hydraulic loading must be inferred. These deviations do not, however, undermine the overall suitability of the model as a framework for linking hydraulic conditions to retention.

These results have several implications for wetland design and management. Design measures that increase V_{eff} and hydraulic efficiency can enhance retention at low to moderate flows and reduce the risk of remobilisation during low flow situations. The strong influence of accumulated, P-rich sediments on event-scale exports highlights the need for active sediment management, including periodic removal from the inlet basin and, where feasible, selected parts of the shallow vegetated zone. The robust performance of turbidity as a TP proxy, in contrast to the weaker DOC and nitrate proxies, suggests that high-frequency monitoring in small wetlands should focus on a limited set of well-calibrated, quality-controlled sensors rather than on many parameters with high uncertainty. Additional dissolved oxygen data which were available from the sensor could give further insight into wetland behaviour in between events during low HL.

More broadly, the study confirmed that small, constructed wetlands in intensively farmed, clay-dominated catchments can provide substantial TP retention, but that their effectiveness is strongly state-dependent and controlled by short-term hydrological variability. HF monitoring combined with a simple hydrological model is therefore not just a technical refinement. It is a necessary basis for identifying when the wetland functions is a reliable nutrient sink and when it behaves as a temporary storage system. This kind of process-level insight will become increasingly important for designing resilient wetland systems and for supporting adaptive nutrient-management strategies under changing climate and changing flow regimes.

References

Bieroza, M.; Acharya, S.; Benisch, J.; ter Borg, R. N.; Hallberg, L.; Negri, C.; Pruitt, A.; Pucher, M.; Saavedra, F.; Staniszewska, K.; van't Veen, S. G. M.; Vincent, A.; Winter, C.; Basu, N. B.; Jarvie, H. P.; Kirchner, J. W. (2023). Advances in Catchment Science, Hydrochemistry, and Aquatic Ecology Enabled by High-Frequency Water Quality Measurements. Environmental Science & Technology 2023, 57, 4701–4719. https://doi.org/10.1021/acs.est.2c07798

Braskerud, B.C. (2002). Factors affecting phosphorus retention in small constructed wetlands treating agricultural non-point source pollution. Ecological Engineering, 19(1), 41–61. https://doi.org/10.1016/S0925-8574(02)00014-9

European Commission (2024). The Water Framework Directive and its implementation. European Commission, Brussels. https://environment.ec.europa.eu/water/water-framework-directive_en

Gericke, O.J. & Smithers, J.C. (2013). Review of methods used to estimate catchment response time for the purpose of peak discharge estimation. *Hydrological Sciences Journal*, 59(11), 1935-1971. https://doi.org/10.1080/02626667.2013.866712

HELCOM (2023). State of the Baltic Sea – Summary report 2023. Helsinki Commission, Helsinki. https://helcom.fi/baltic-sea-trends/holistic-assessments/state-of-the-baltic-sea-2023/

Hoffmeister, S., Murphy, K.R., Cascone, C., Ledesma, J.L.J. and Köhler, S.J. (2020) 'Evaluating the accuracy of two in situ optical sensors to estimate dissolved organic carbon concentrations in rivers', Environmental Science: Water Research & Technology, 6(10), 2891–2901. https://doi.org/10.1039/D0EW00150C

Jarvie, H.P., Pallett, D.W., Schäfer, S.M., Macrae, M.L., Bowes, M.J., Farrand, P., Warwick, A.C., King, S.M., Williams, R.J., Armstrong, L., Nicholls, D.J.E., Lord, W.D., Rylett, D., Roberts, C. & Fisher, N. (2020). Biogeochemical and climate drivers of wetland phosphorus and nitrogen release: Implications for nutrient legacies and eutrophication risk. Journal of Environmental Quality, 49(6), 1703–1716. https://doi.org/10.1002/jeq2.20155

Jones, A.S., Stevens, D.K., Horsburgh, J.S. and Mesner, N.O. (2011). Surrogate measures for providing high frequency estimates of total suspended solids and total phosphorus concentrations. JAWRA Journal of the American Water Resources Association, 47(2), 239–253. https://doi.org/10.1111/j.1752-1688.2010.00505.x

Kadlec, R.H. and Wallace, S.D. (2009). *Treatment Wetlands*. 2nd ed. CRC Press, Boca Raton. https://doi.org/10.1201/9781420012514

Koskiaho, J., & Puustinen, M. (2019). Suspended solids and nutrient retention in two constructed wetlands as determined from continuous data recorded with sensors. Ecological Engineering, 137, 65–75. https://doi.org/10.1016/j.ecoleng.2019.04.006

Kynkäänniemi, P. (2014). Small wetlands designed for phosphorus retention in Swedish agricultural areas: Efficiency variations during the first years after construction. Doctoral thesis 2014:70. Swedish University of Agricultural Sciences, Uppsala. http://pub.epsilon.slu.se/11471/

Land, M., Granéli, W., Grimvall, A., Hoffmann, C.C., Mitsch, W.J., Tonderski, K.S. and Verhoeven, J.T.A. (2016) 'How effective are created or restored freshwater wetlands for nitrogen and phosphorus removal? A systematic review', Environmental Evidence, 5, 9. https://doi.org/10.1186/s13750-016-0060-0

Lannergård, E. (2016). Potential for using high-frequency turbidity as a proxy for total phosphorus in rivers and streams. Master's thesis. Swedish University of Agricultural Sciences (SLU), Uppsala.

Lannergård, E.E., Ledesma, J.L.J., Fölster, J. and Futter, M.N. (2019) An evaluation of high frequency turbidity as a proxy for riverine total phosphorus concentrations, Science of the Total Environment, 651, 1037–1048. https://doi.org/10.1016/j.scitotenv.2018.09.127

Lannergård, E.E., Fölster, J. and Futter, M.N. (2021) Turbidity-discharge hysteresis in a meso-scale catchment: The importance of intermediate scale events, Hydrological Processes, 35(12), e14435. https://doi.org/10.1002/hyp.14435

Lee, E.J.; Yoo, G.Y.; Jeong, Y.; Kim, K.U.; Park, J.H.; Oh, N.H. (2015) Comparison of UV–VIS and FDOM Sensors for In Situ Monitoring of Stream DOC Concentrations. *Biogeosciences* 2015,*12*, 3109–3118. https://doi.org/10.5194/bg-12-3109-2015

Mendes, L.R.D. (2020). Edge-of-field technologies for phosphorus retention from agricultural drainage discharge. Applied Sciences, 10(19), 7004. https://doi.org/10.3390/app10020634

Moatar, F., Abbott, B.W., Minaudo, C., Curie, F. and Pinay, G. (2017). Elemental properties, hydrology, and biology interact to shape concentration–discharge curves for carbon, nutrients, sediment, and major ions. Water Resources Research, 53(2), 1270–1287. https://doi.org/10.1002/2016WR019635

Pellerin, B.A., Bergamaschi, B.A., Downing, B.D., Saraceno, J.F., Garrett, J.D. and Olsen, L.D. (2016). Optical techniques for the determination of nitrate in environmental waters: guidelines for instrument selection, operation, deployment, maintenance, quality assurance, and data reporting. U.S. Geological Survey Techniques and Methods, book 1, chap. D5. https://doi.org/10.3133/tm1D5

Persson, J., Somes, N.L.G. and Wong, T.H.F. (1999). Hydraulics efficiency of constructed wetlands and ponds. Water Science and Technology, 40(3), 291–300. https://doi.org/10.2166/wst.1999.0174

Rode, M.; Wade, A. J.; Cohen, M. J.; Hensley, R. T.; Bowes, M. J.; Kirchner, J. W.; Arhonditsis, G. B.; Jordan, P.; Kronvang, B.; Halliday, S. J.; Skeffington, R. A.; Rozemeijer, J. C.; Aubert, A. H.; Rinke, K.; Jomaa, S. (2016). Sensors in the Stream: The High-Frequency Wave of the Present. Environmental Science & Technology 2016, 50, 10297–10307. https://doi.org/10.1021/acs.est.6b02155

SMHI (Swedish Meteorological and Hydrological Institute). (2026) Meteorological observations. https://www.smhi.se

Smith, E., Gordon, R., Madani, A., Stratton, G. (2005). Cold climate hydrological flow characteristics of constructed wetlands. *Canadian Biosystems Engineering*, 47, 1.1–1.7. DOI: none assigned

Ulén, B., Geranmayeh, P., Blomberg, M. and Bieroza, M. (2019). Seasonal variation in nutrient retention in a free water surface constructed wetland monitored with flow-proportional sampling and optical sensors. Ecological Engineering, 139, 105588. https://doi.org/10.1016/j.ecoleng.2019.105588

USDA Natural Resources Conservation Service. (2010). Part 630 Hydrology: Chapter 15, Time of Concentration. National Engineering Handbook. Washington, DC: USDA NRCS.

https://irrigationtoolbox.com/NEH/Part630_Hydrology/NEH630-ch15draft.pdf. DOI: none assigned

van't Veen, S.G.M., Kronvang, B., Audet, J., Davidson, T.A., Jeppesen, E., Kristensen, E.A., Larsen, S.E., Laugesen, J.R., Levi, E.E., Nielsen, A. and Andersen, P.M. (2025). SentemQC – A novel and cost-efficient method for quality assurance and quality control of high-resolution sensor data in fresh waters. Open Research Europe, 4, 244. https://doi.org/10.12688/openreseurope.18134.2

Vaughan, M.C.H., Bowden, W.B., Shanley, J.B., Vermilyea, A.W., Sleeper, R., Gold, A.J., Pradhanang, S.M., Inamdar, S.P., Levia, D.F., Andres, A.S., Birgand, F. and Schroth, A.W. (2017). High-frequency dissolved organic carbon and nitrate measurements reveal differences in storm hysteresis and loading in relation to land cover and seasonality. Water Resources Research, 53(7), 5345–5363. https://doi.org/10.1002/2017WR020491

Villa, A., Fölster, J. and Kyllmar, K. (2019). Determining suspended solids and total phosphorus from turbidity: comparison of high-frequency sampling with conventional monitoring methods. Environmental Monitoring and Assessment, 191, 605. https://doi.org/10.1007/s10661-019-7775-7

Wahl, M.D., Brown, L.C., Soboyejo, A.O., Dong, B. & Li, X. (2010). Establishing a relationship between hydraulic efficiency and treatment performance in constructed wetlands. In: XVIIth World Congress of the International Commission of Agricultural and Biosystems Engineering (CIGR), Québec City, Canada, June 13–17, 2010. https://10.13031/2013.32172

YSI Inc. (2012). EXO User Manual: Water Quality Sondes EXO1, EXO2 and EXO3. YSI Inc., Yellow Springs, OH. https://www.ysi.com/file%20library/documents/manuals/exo-user-manual-web.pdf

Popular science summary

Farming needs nutrients such as phosphorus to produce food. When too much phosphorus is washed from fields into streams, rivers, and the Baltic Sea, it can cause algal blooms and lack of oxygen in the water. This is bad for fish, plants, and people who want clean water. One way to limit these losses is to build small wetlands at the edge of fields so that the water has to pass through them before it reaches a stream.

The wetland in this study is located at Nybble in east-central Sweden. It was built to trap phosphorus coming from a small clay-soil catchment with tile drains and arable land. The wetland is shallow and narrow, with plants that slow the water and help fine particles settle on the bottom. Earlier studies showed that it stores large amounts of phosphorus-rich sediment, but they could not fully explain what happens during short, intense runoff events such as rain on wet soil or snowmelt.

To study this in more detail, high-frequency sensors were installed at the inlet and outlet of the wetland. These instruments measured water level, temperature, oxygen, and two important optical signals: turbidity, which shows how many particles are in the water, and fluorescent dissolved organic matter (fDOM), which is related to dissolved organic carbon. Measurements were taken every 15 minutes from late autumn to spring. At the same time, water samples were collected every two weeks and analysed in the laboratory for total phosphorus, dissolved organic carbon, and other substances. The laboratory data were then used for calibration to use the sensor signals so they could be translated into continuous concentration and load estimates.

The results show that turbidity is a reliable proxy for total phosphorus in this wetland. When turbidity increased, total phosphorus in the water also increased in a clear and almost linear way. This made it possible to calculate phosphorus loads for every hour and every event, something that would be very costly and impractical with laboratory samples alone. In contrast, the relationship between fDOM and dissolved organic carbon was much weaker, and a separate nitrate sensor did not work well because it drifted over time, so nitrogen dynamics could not be analysed.

During most runoff events, the wetland acted as a sink for phosphorus: more phosphorus entered than left. Retention was especially strong at moderate flow conditions, when water was fast enough to bring particles into the wetland but still slow enough for them to settle. However, the study also found periods with little or even negative retention. Under very low flow, when throughflow was small, the wetland sometimes released phosphorus that had been stored in surface sediments. Short episodes of export were also seen at the start of some events, when rising water levels likely stirred up fine material from the bottom.

These findings show that a small, constructed wetland is not simply a constant filter that always traps the same share of phosphorus. Instead, its behaviour changes with the flow conditions. It usually helps reduce phosphorus losses from the catchment, but it can also act as a temporary source when stored sediment is mobilised. High-frequency monitoring is therefore a powerful tool for understanding when the wetland works as intended and when it does not. This knowledge can support better design and management, for example by guiding when and where to remove accumulated sediment so that the wetland continues to protect downstream waters in a changing climate.

Appendix

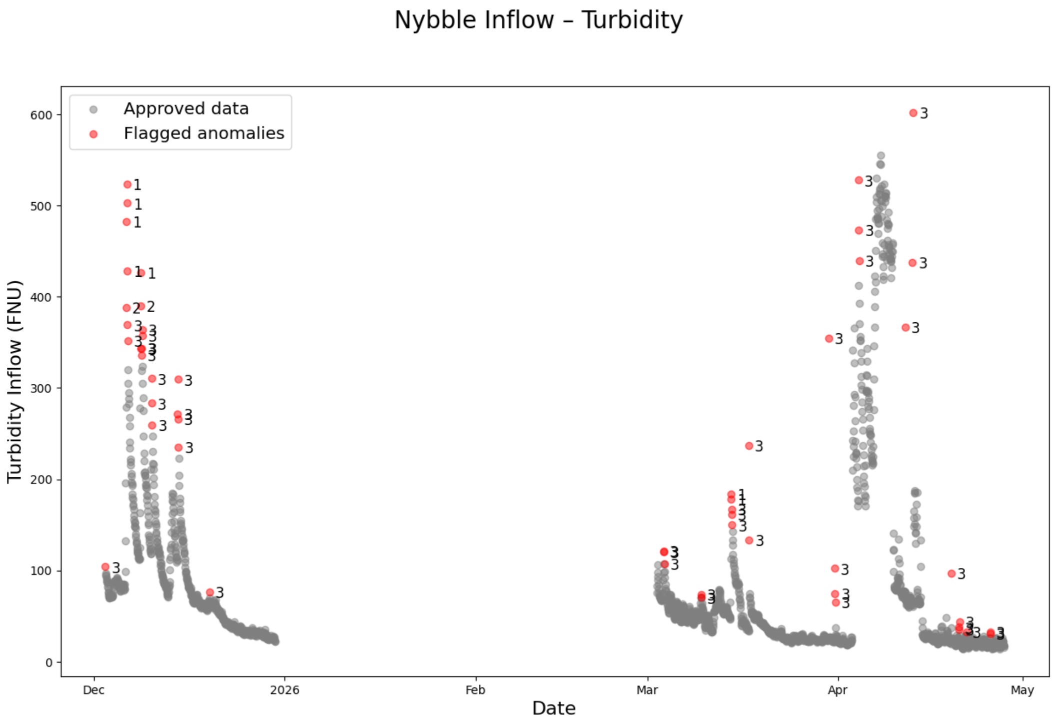

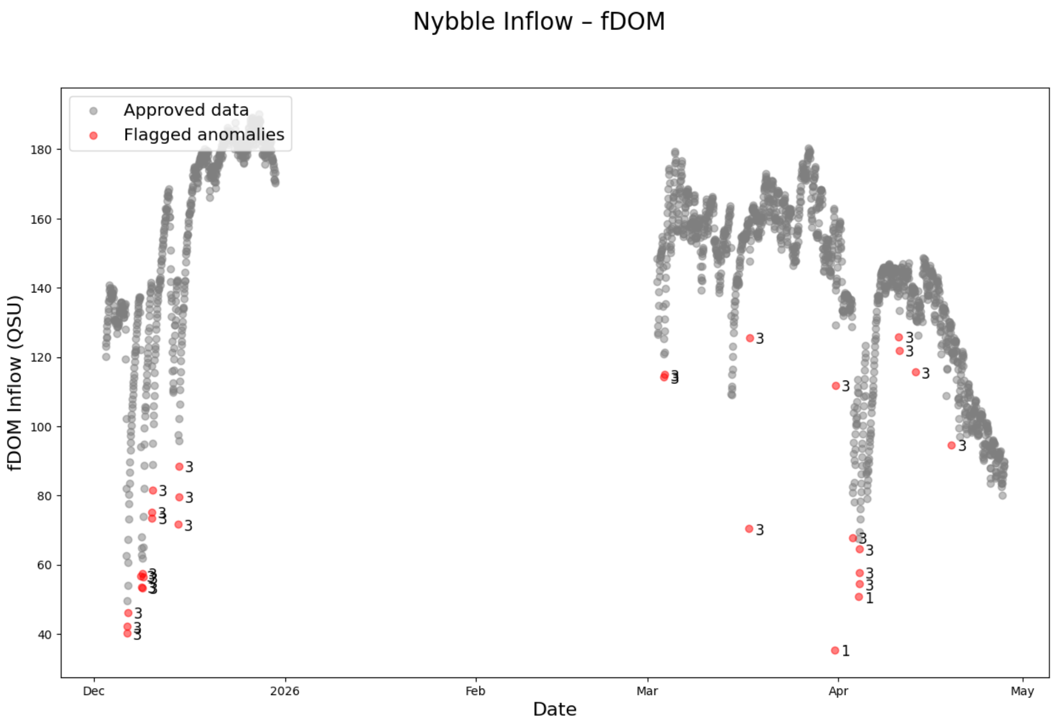

Figure 10 - Inflow data analysis, flagged anomalies are indicated by the red dots

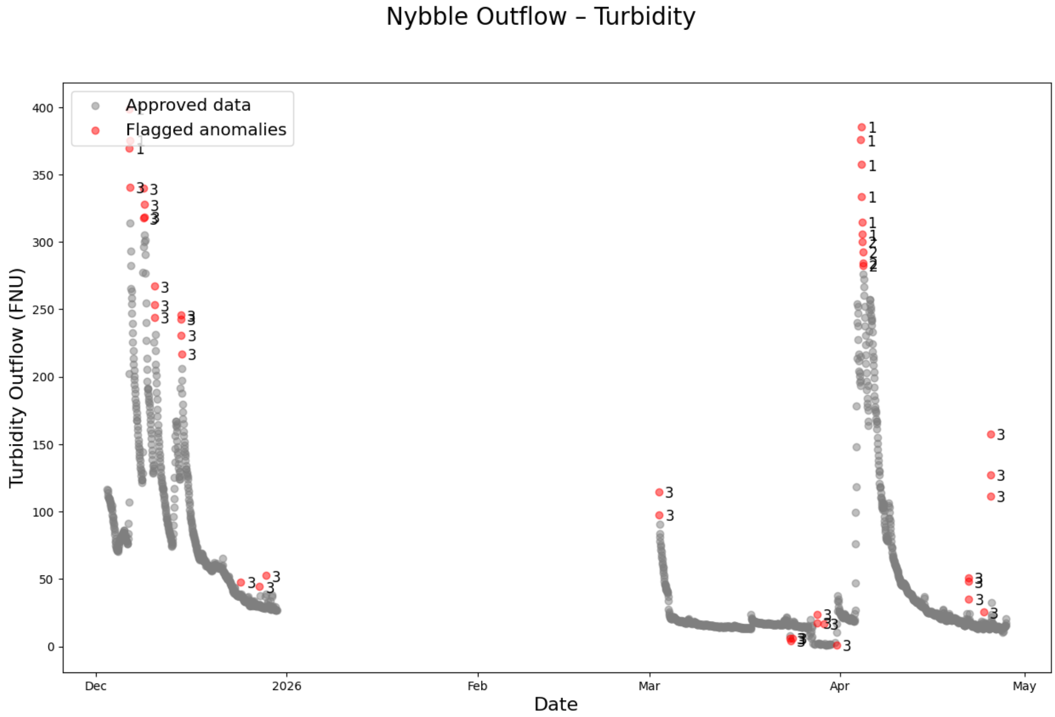

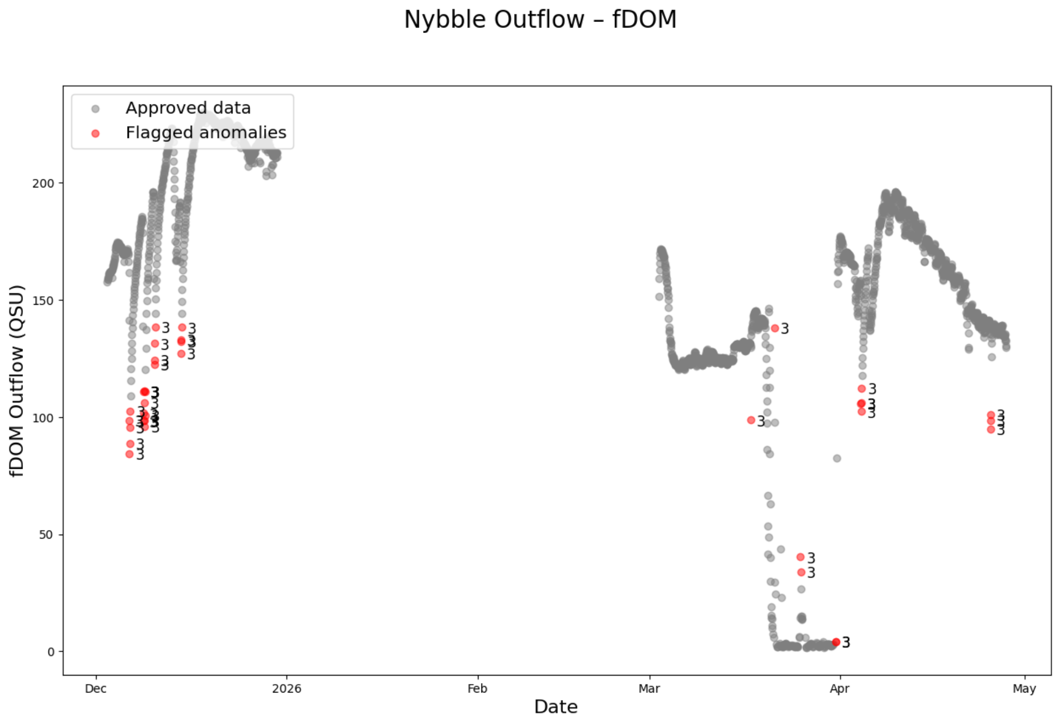

Figure 11 - Outflow Data Analysis, flagged anomalies are indicated by the red dot

Figure 12 - Untreated 15min interval Nitrate readings from NitraLED sensor (above) and zoomed in (below). Observations are indicated as dots for inflow (violett) outflow (pink)

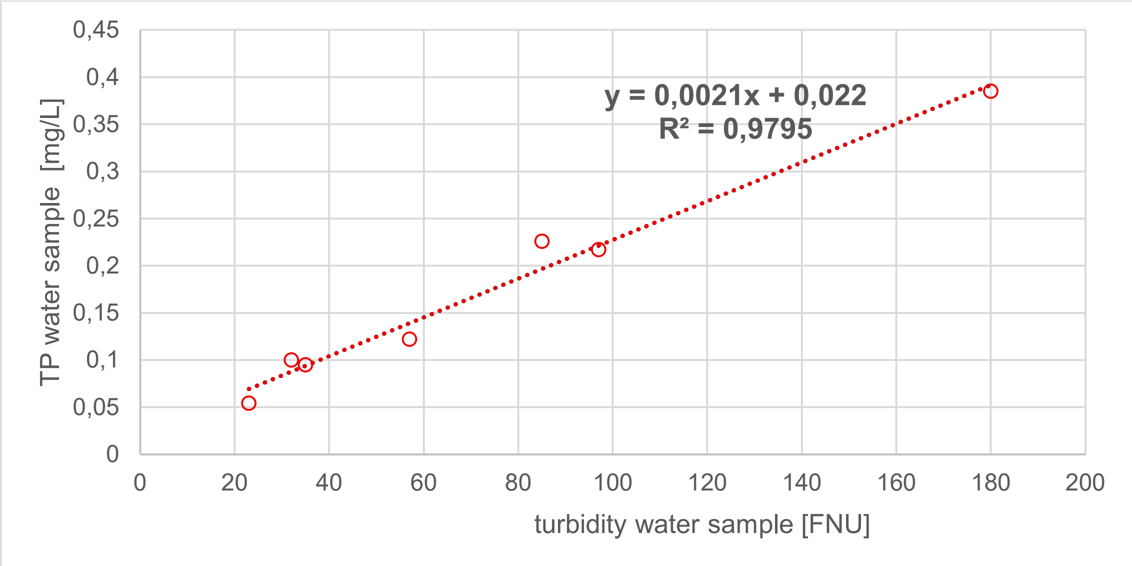

Figure 13 - Inlet Calibration of turbidity (FNU) against TP (n=7) Observations are indicated by the red dots and regression line (red dotted).

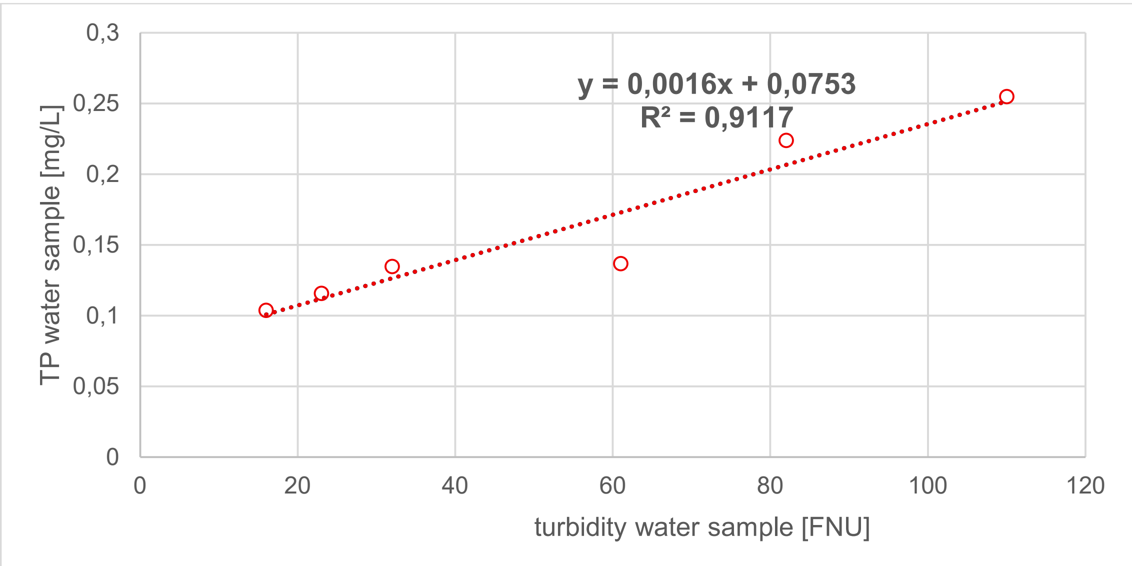

Figure 14 - Outlet Calibration of turbidity water samples against TP from water samples (n=6). Observations are indicated by the red dots and regression line (red dotted).

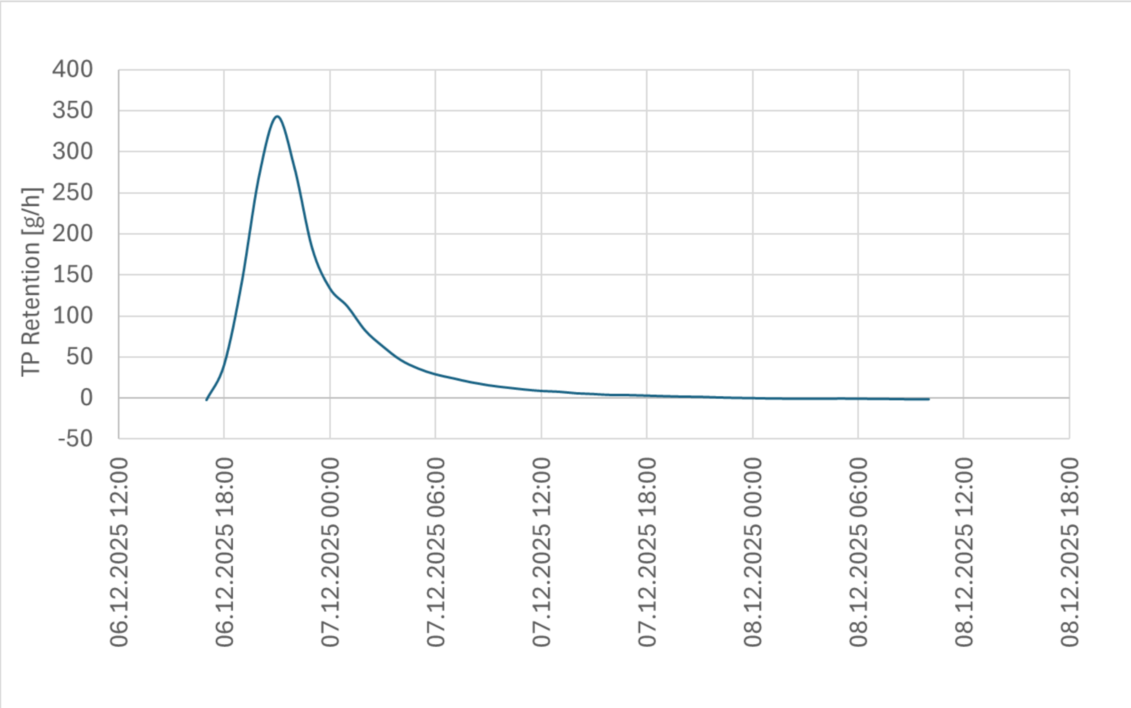

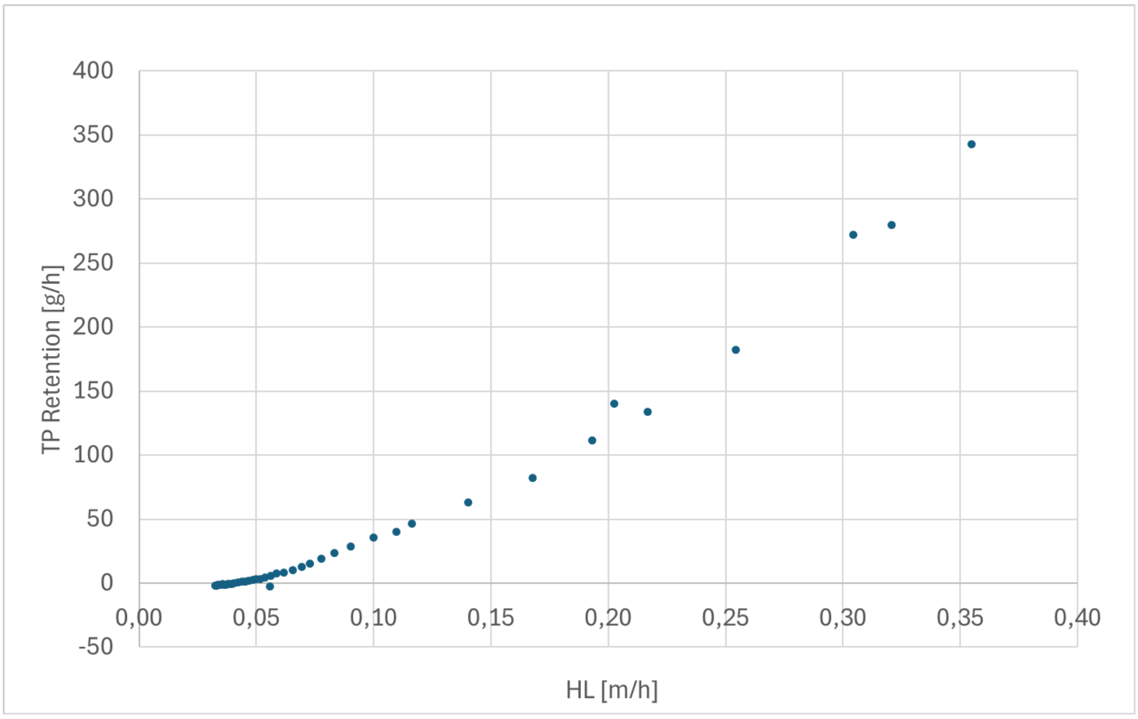

Figure 15 - Event 1; Event-scale phosphorus retention, shown as (top) temporal dynamics of retention rate and (bottom) relationship between event-specific retention rate and hydraulic load (HL) measured during the same period considering the time lag.

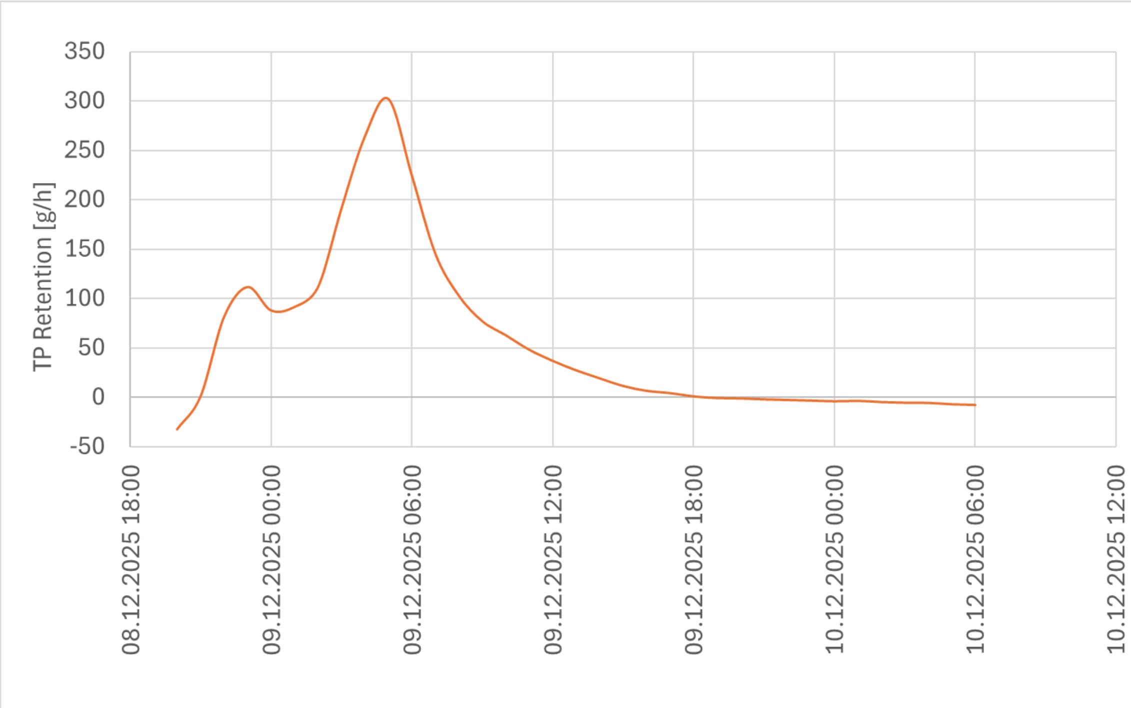

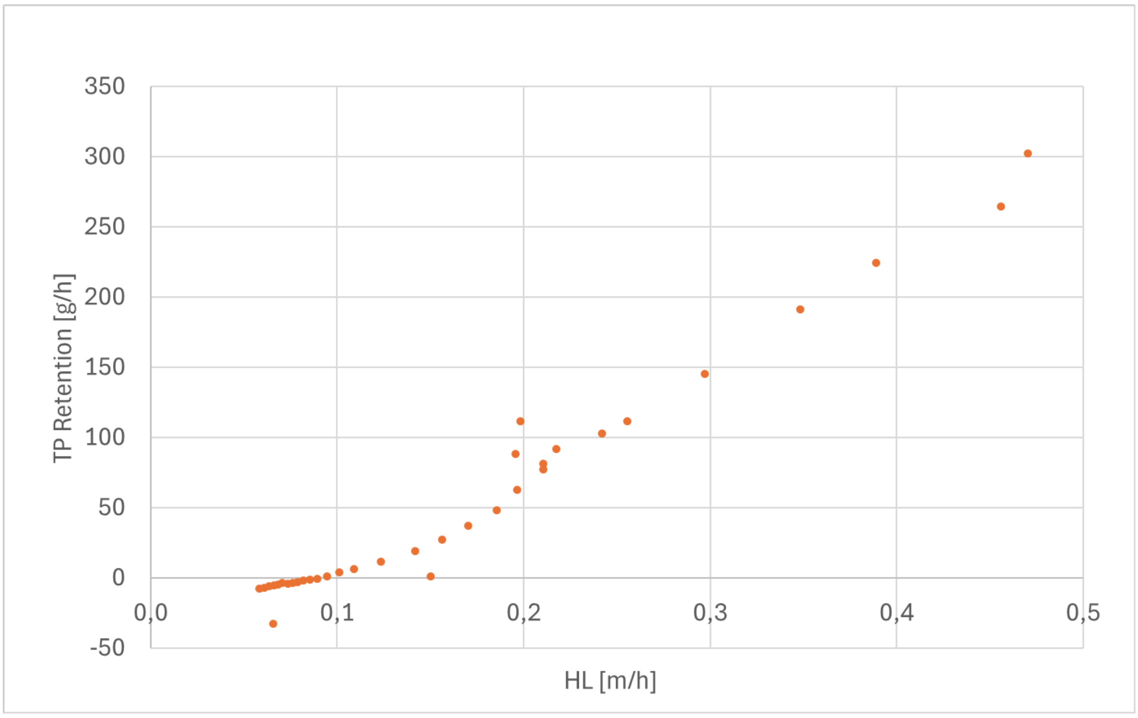

Figure 16 - Event 2; Event-scale phosphorus retention, shown as (top) temporal dynamics of retention rate and (bottom) relationship between event-specific retention rate and hydraulic load (HL) measured during the same period considering the time lag.

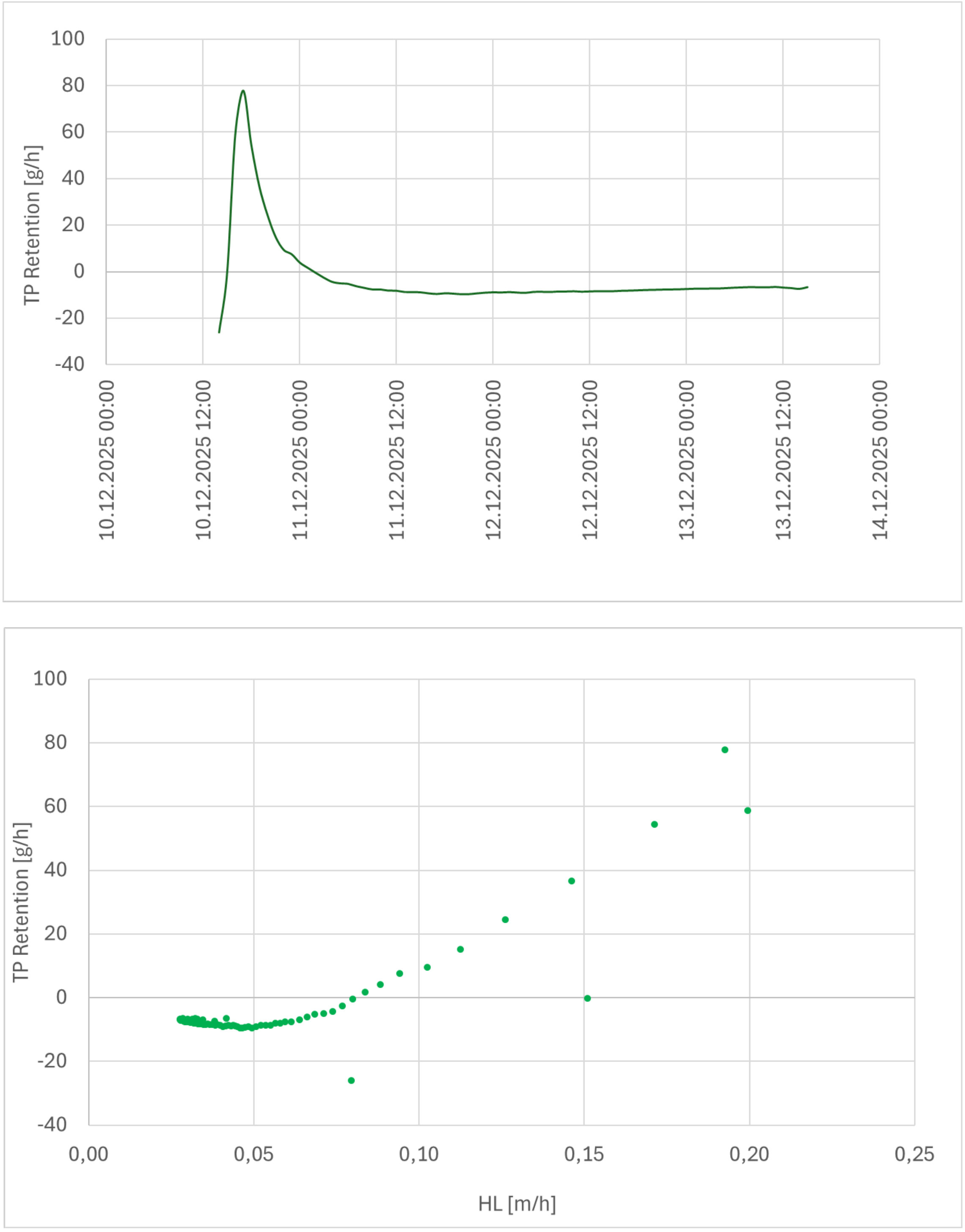

Figure 17 - Event 3; Event-scale phosphorus retention, shown as (top) temporal dynamics of retention rate and (bottom) relationship between event-specific retention rate and hydraulic load (HL) measured during the same period considering the time lag.

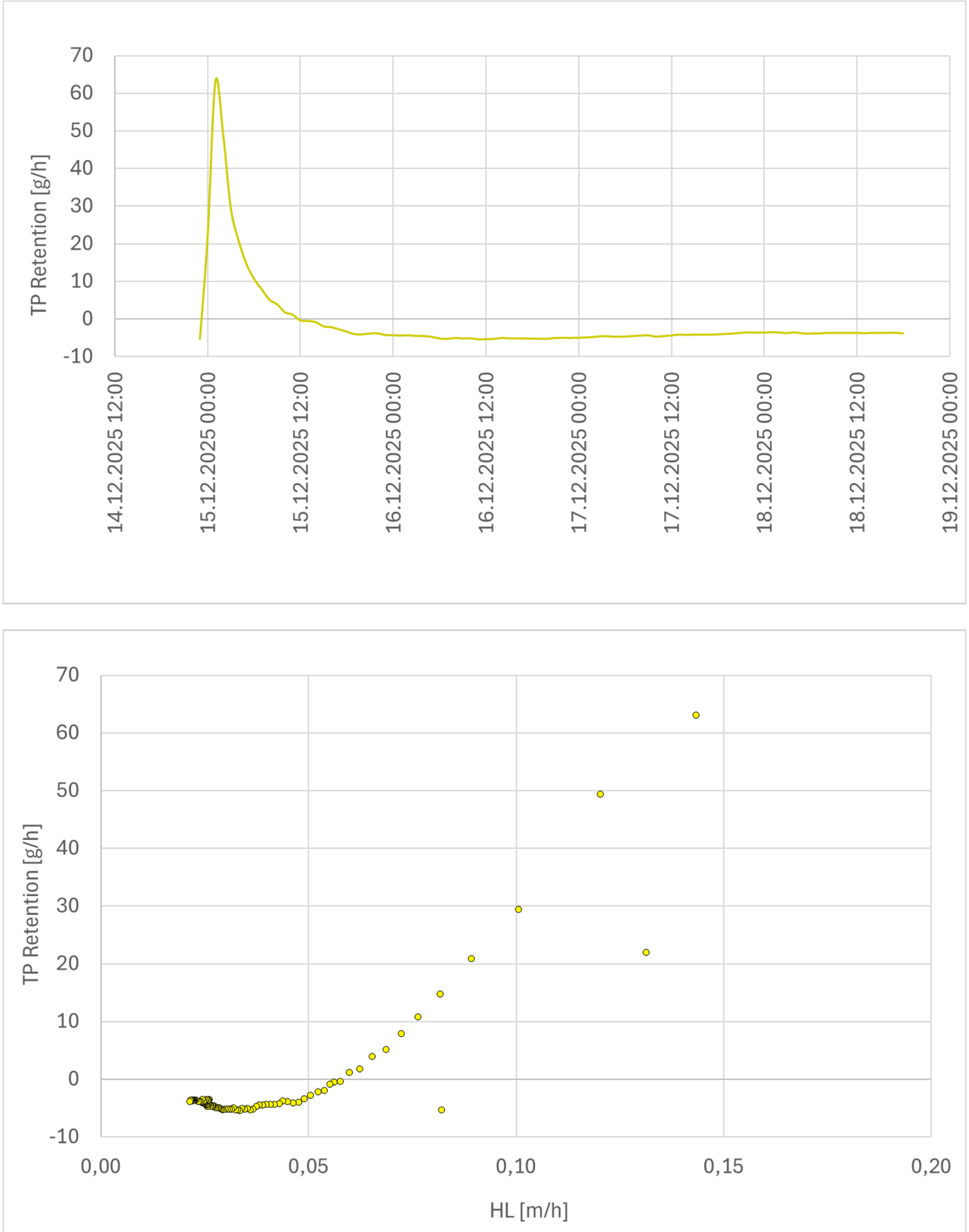

Figure 18 - Event 4; Event-scale phosphorus retention, shown as (top) temporal dynamics of retention rate and (bottom) relationship between event-specific retention rate and hydraulic load (HL) measured during the same period considering the time lag.

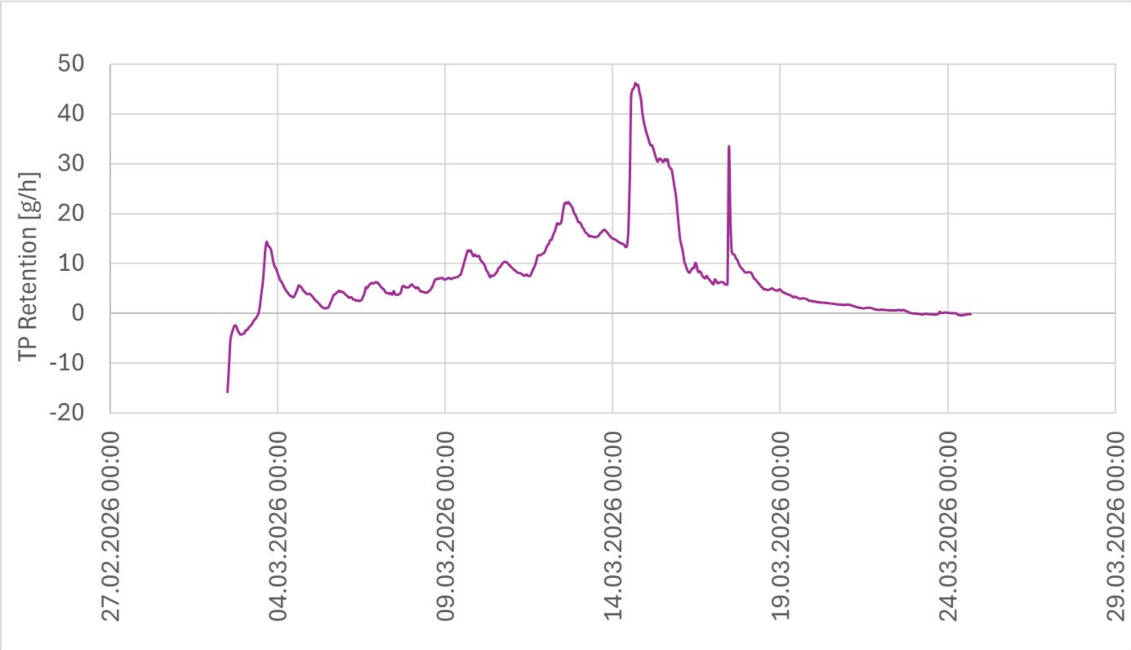

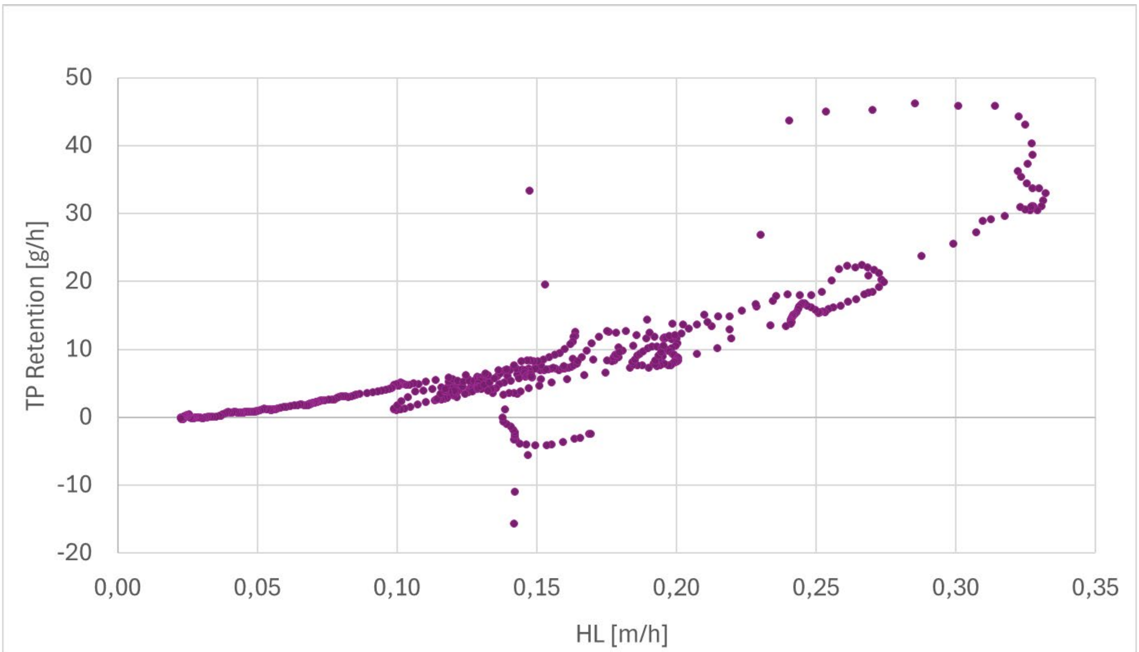

Figure 19 - Event 5; Event-scale phosphorus retention, shown as (top) temporal dynamics of retention rate and (bottom) relationship between event-specific retention rate and hydraulic load (HL) measured during the same period considering the time lag.

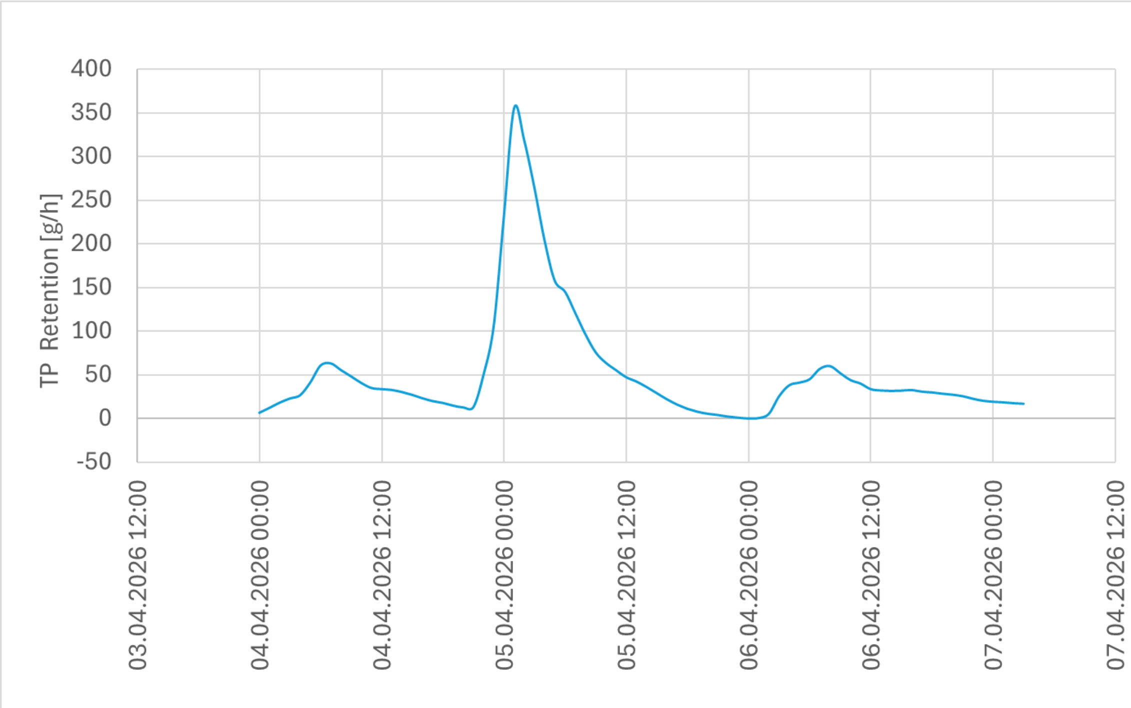

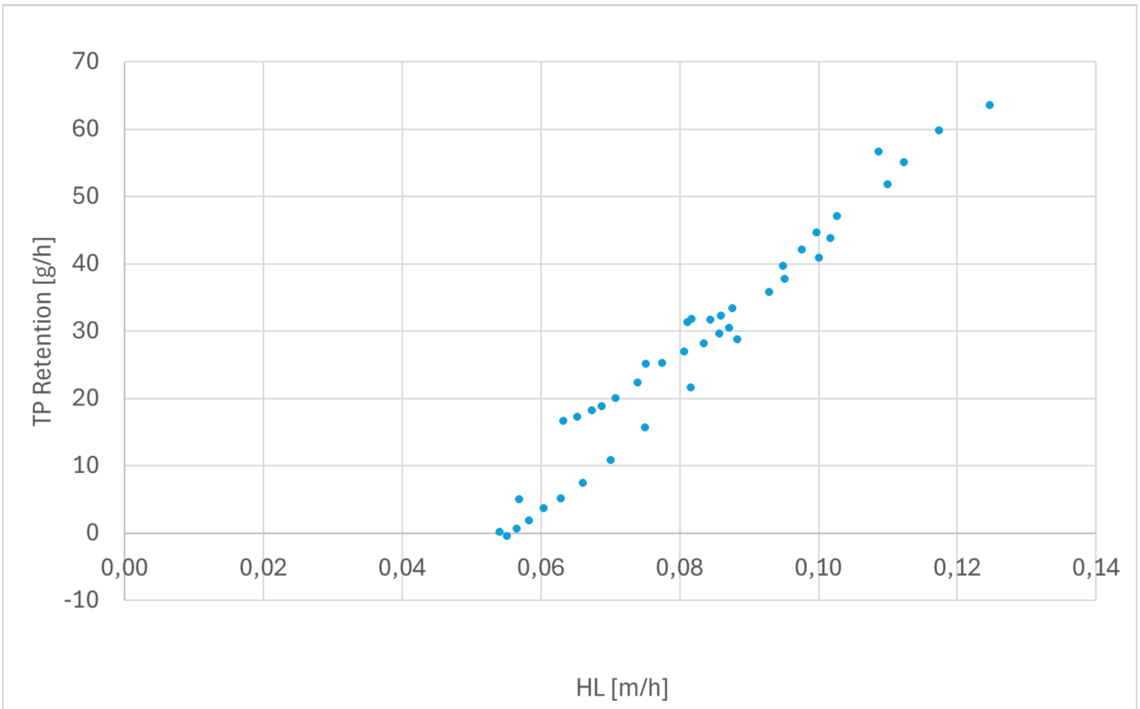

Figure 20 - Event 6; Event-scale phosphorus retention, shown as (top) temporal dynamics of retention rate and (bottom) relationship between event-specific retention rate and hydraulic load (HL) measured during the same period considering the time lag.

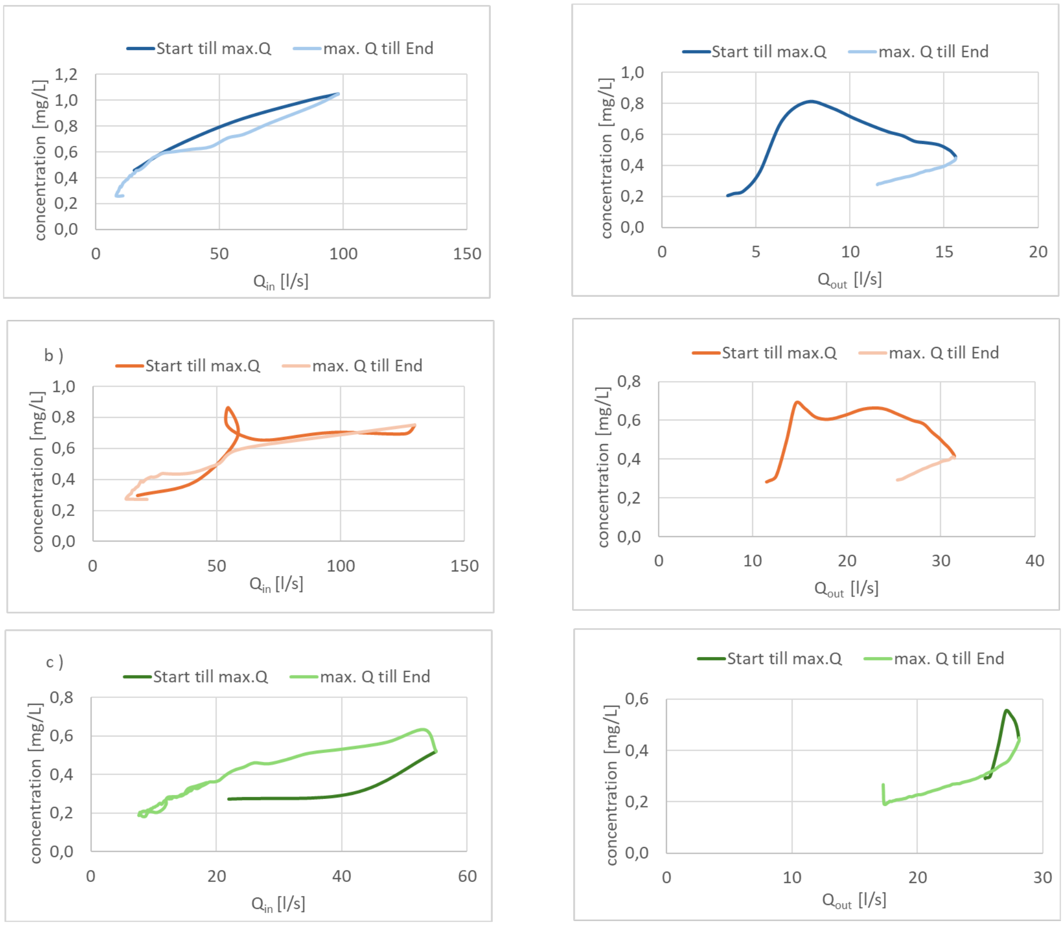

Figure 21 - Flow–concentration hysteresis of event-scale TP concentrations as a function of discharge for three runoff events a) blue = Event 1, b) orange = Event 2, c) green = Event 3) at the inlet (left) and outlet (right); darker lines indicate the rising limb (start to peak flow), lighter lines the falling limb (peak flow to end of event).

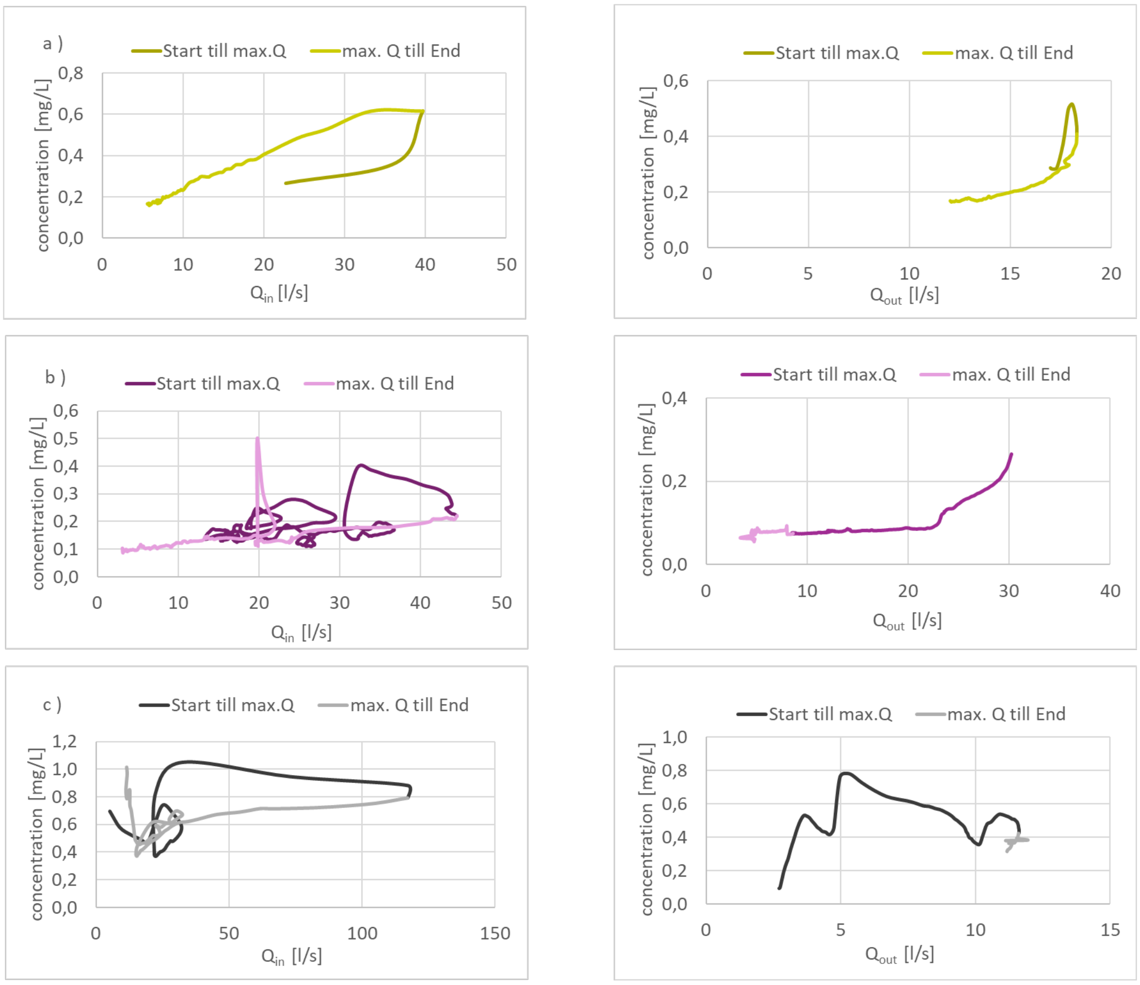

Figure 22 - Flow–concentration hysteresis of event-scale TP concentrations as a function of discharge for three runoff events a) yellow = Event 4, b) purple = Event 5, c) grey = Event 6 at the inlet (left) and outlet (right); darker lines indicate the rising limb (start to peak flow), lighter lines the falling limb (peak flow to end of event).

Publishing and archiving

Approved students' theses at SLU can be published online. As a student you own the copyright to your work and in such cases, you need to approve the publication. In connection with your approval of publication, SLU will process your personal data (name) to make the work searchable on the internet. You can revoke your consent at any time by contacting the library.

Even if you choose not to publish the work or if you revoke your approval, the thesis will be archived digitally according to archive legislation.

You will find links to SLU's publication agreement and SLU's processing of personal data and your rights on this page:

- https://libanswers.slu.se/en/faq/228318

☒ YES, I, Matthias Nikel, have read and agree to the agreement for publication and the personal data processing that takes place in connection with this

☐ NO, I/we do not give my/our permission to publish the full text of this work. However, the work will be uploaded for archiving and the metadata and summary will be visible and searchable.